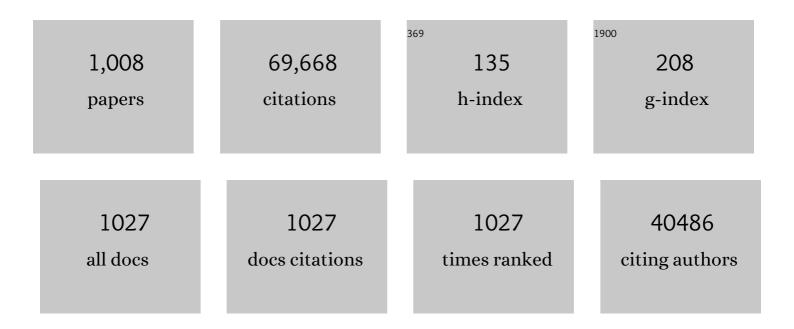
List of Publications by Year in descending order

Source: https://exaly.com/author-pdf/2516123/publications.pdf Version: 2024-02-01



HUA KUN LUI

#	Article	IF	CITATIONS
1	Enhancement of the critical current density and flux pinning of MgB2 superconductor by nanoparticle SiC doping. Applied Physics Letters, 2002, 81, 3419-3421.	3.3	770
2	Preparation and Electrochemical Properties of SnO2 Nanowires for Application in Lithium-Ion Batteries. Angewandte Chemie - International Edition, 2007, 46, 750-753.	13.8	756
3	Extension of The Stöber Method to the Preparation of Monodisperse Resorcinol–Formaldehyde Resin Polymer and Carbon Spheres. Angewandte Chemie - International Edition, 2011, 50, 5947-5951.	13.8	745
4	Highly Reversible Lithium Storage in Spheroidal Carbon-Coated Silicon Nanocomposites as Anodes for Lithium-Ion Batteries. Angewandte Chemie - International Edition, 2006, 45, 6896-6899.	13.8	656
5	Boosted Charge Transfer in SnS/SnO ₂ Heterostructures: Toward High Rate Capability for Sodiumâ€ion Batteries. Angewandte Chemie - International Edition, 2016, 55, 3408-3413.	13.8	621
6	Enhanced Sodium-Ion Battery Performance by Structural Phase Transition from Two-Dimensional Hexagonal-SnS ₂ to Orthorhombic-SnS. ACS Nano, 2014, 8, 8323-8333.	14.6	592
7	Metalâ€Free Carbon Materials for CO ₂ Electrochemical Reduction. Advanced Materials, 2017, 29, 1701784.	21.0	558
8	Superior stability and high capacity of restacked molybdenum disulfide as anode material for lithium ion batteries. Chemical Communications, 2010, 46, 1106-1108.	4.1	527
9	In situ chemical synthesis of SnO2–graphene nanocomposite as anode materials for lithium-ion batteries. Electrochemistry Communications, 2009, 11, 1849-1852.	4.7	520
10	Sodiumâ€ion Batteries: From Academic Research to Practical Commercialization. Advanced Energy Materials, 2018, 8, 1701428.	19.5	494
11	Reduced graphene oxide with superior cycling stability and rate capability for sodium storage. Carbon, 2013, 57, 202-208.	10.3	491
12	Electrodeposition of MnO2 nanowires on carbon nanotube paper as free-standing, flexible electrode for supercapacitors. Electrochemistry Communications, 2008, 10, 1724-1727.	4.7	419
13	Comparison of GO, GO/MWCNTs composite and MWCNTs as potential electrode materials for supercapacitors. Energy and Environmental Science, 2011, 4, 1855.	30.8	414
14	Transition metal based battery-type electrodes in hybrid supercapacitors: A review. Energy Storage Materials, 2020, 28, 122-145.	18.0	413
15	Enhanced reversible lithium storage in a nanosize silicon/graphene composite. Electrochemistry Communications, 2010, 12, 303-306.	4.7	402
16	Grapheneâ€Encapsulated Fe ₃ O ₄ Nanoparticles with 3D Laminated Structure as Superior Anode in Lithium Ion Batteries. Chemistry - A European Journal, 2011, 17, 661-667.	3.3	395
17	CoS Quantum Dot Nanoclusters for Highâ€Energy Potassiumâ€lon Batteries. Advanced Functional Materials, 2017, 27, 1702634.	14.9	391
18	Simply Mixed Commercial Red Phosphorus and Carbon Nanotube Composite with Exceptionally Reversible Sodium-Ion Storage. Nano Letters, 2013, 13, 5480-5484.	9.1	390

#	Article	IF	CITATIONS
19	Recent Progress in Graphite Intercalation Compounds for Rechargeable Metal (Li, Na, K, Al)â€lon Batteries. Advanced Science, 2017, 4, 1700146.	11.2	390
20	Uniform yolk-shell iron sulfide–carbon nanospheres for superior sodium–iron sulfide batteries. Nature Communications, 2015, 6, 8689.	12.8	374
21	Rapid Synthesis of Li ₄ Ti ₅ O ₁₂ Microspheres as Anode Materials and Its Binder Effect for Lithium-Ion Battery. Journal of Physical Chemistry C, 2011, 115, 16220-16227.	3.1	368
22	Sulfur-graphene composite for rechargeable lithium batteries. Journal of Power Sources, 2011, 196, 7030-7034.	7.8	362
23	Sulfur–mesoporous carbon composites in conjunction with a novel ionic liquid electrolyte for lithium rechargeable batteries. Carbon, 2008, 46, 229-235.	10.3	361
24	Small things make a big difference: binder effects on the performance of Li and Na batteries. Physical Chemistry Chemical Physics, 2014, 16, 20347-20359.	2.8	347
25	Atomic Interface Engineering and Electricâ€Field Effect in Ultrathin Bi ₂ MoO ₆ Nanosheets for Superior Lithium Ion Storage. Advanced Materials, 2017, 29, 1700396.	21.0	343
26	Amorphous TiO ₂ Shells: A Vital Elastic Buffering Layer on Silicon Nanoparticles for Highâ€Performance and Safe Lithium Storage. Advanced Materials, 2017, 29, 1700523.	21.0	342
27	Lithiumâ€ion Conducting Electrolyte Salts for Lithium Batteries. Chemistry - A European Journal, 2011, 17, 14326-14346.	3.3	341
28	Synthesis of molybdenum disulfide (MoS2) for lithium ion battery applications. Materials Research Bulletin, 2009, 44, 1811-1815.	5.2	339
29	Regulation methods for the Zn/electrolyte interphase and the effectiveness evaluation in aqueous Zn-ion batteries. Energy and Environmental Science, 2021, 14, 5669-5689.	30.8	314
30	Synthesis of NiO nanotubes for use as negative electrodes in lithium ion batteries. Journal of Power Sources, 2006, 159, 254-257.	7.8	312
31	Active-Site-Enriched Iron-Doped Nickel/Cobalt Hydroxide Nanosheets for Enhanced Oxygen Evolution Reaction. ACS Catalysis, 2018, 8, 5382-5390.	11.2	311
32	The Effect of Morphological Modification on the Electrochemical Properties of SnO ₂ Nanomaterials. Advanced Functional Materials, 2008, 18, 455-461.	14.9	306
33	Flexible free-standing carbon nanotube films for model lithium-ion batteries. Carbon, 2009, 47, 2976-2983.	10.3	306
34	Atomic cobalt as an efficient electrocatalyst in sulfur cathodes for superior room-temperature sodium-sulfur batteries. Nature Communications, 2018, 9, 4082.	12.8	305
35	Hollow Structured Li ₃ VO ₄ Wrapped with Graphene Nanosheets in Situ Prepared by a One-Pot Template-Free Method as an Anode for Lithium-Ion Batteries. Nano Letters, 2013, 13, 4715-4720.	9.1	303
36	Hydrogen Storage Materials for Mobile and Stationary Applications: Current State of the Art. ChemSusChem, 2015, 8, 2789-2825.	6.8	302

#	Article	IF	CITATIONS
37	Sn _{4+<i>x</i>} P ₃ @ Amorphous Snâ€P Composites as Anodes for Sodiumâ€lon Batteries with Low Cost, High Capacity, Long Life, and Superior Rate Capability. Advanced Materials, 2014, 26, 4037-4042.	21.0	298
38	Monodisperse Magnesium Hydride Nanoparticles Uniformly Selfâ€Assembled on Graphene. Advanced Materials, 2015, 27, 5981-5988.	21.0	298
39	Ultrafine SnO ₂ nanoparticle loading onto reduced graphene oxide as anodes for sodium-ion batteries with superior rate and cycling performances. Journal of Materials Chemistry A, 2014, 2, 529-534.	10.3	297
40	Enhancement of the capacitance in TiO2 nanotubes through controlled introduction of oxygen vacancies. Journal of Materials Chemistry, 2011, 21, 5128.	6.7	288
41	Reversible structural evolution of sodium-rich rhombohedral Prussian blue for sodium-ion batteries. Nature Communications, 2020, 11, 980.	12.8	283
42	Development of MoS ₂ –CNT Composite Thin Film from Layered MoS ₂ for Lithium Batteries. Advanced Energy Materials, 2013, 3, 798-805.	19.5	282
43	Amorphous Carbon Coated High Grain Boundary Density Dual Phase Li ₄ Ti ₅ O ₁₂ â€TiO ₂ : A Nanocomposite Anode Material for Liâ€lon Batteries. Advanced Energy Materials, 2011, 1, 212-220.	19.5	281
44	Achieving High-Performance Room-Temperature Sodium–Sulfur Batteries With S@Interconnected Mesoporous Carbon Hollow Nanospheres. Journal of the American Chemical Society, 2016, 138, 16576-16579.	13.7	280
45	Carbon-coated SnO2/graphene nanosheets as highly reversible anode materials for lithium ion batteries. Carbon, 2012, 50, 1897-1903.	10.3	276
46	Roomâ€Temperature Sodiumâ€Sulfur Batteries: A Comprehensive Review on Research Progress and Cell Chemistry. Advanced Energy Materials, 2017, 7, 1602829.	19.5	270
47	Sulphur-polypyrrole composite positive electrode materials for rechargeable lithium batteries. Electrochimica Acta, 2006, 51, 4634-4638.	5.2	265
48	Single wall carbon nanotube paper as anode for lithium-ion battery. Electrochimica Acta, 2005, 51, 23-28.	5.2	263
49	Catalytic Role of Ge in Highly Reversible GeO ₂ /Ge/C Nanocomposite Anode Material for Lithium Batteries. Nano Letters, 2013, 13, 1230-1236.	9.1	261
50	Highly Reversible and Large Lithium Storage in Mesoporous Si/C Nanocomposite Anodes with Silicon Nanoparticles Embedded in a Carbon Framework. Advanced Materials, 2014, 26, 6749-6755.	21.0	260
51	Activated carbon from the graphite with increased rate capability for the potassium ion battery. Carbon, 2017, 123, 54-61.	10.3	257
52	A study on the charge–discharge mechanism of Co3O4 as an anode for the Li ion secondary battery. Electrochimica Acta, 2005, 50, 3667-3673.	5.2	255
53	Understanding the Reaction Chemistry during Charging in Aprotic Lithium–Oxygen Batteries: Existing Problems and Solutions. Advanced Materials, 2019, 31, e1804587.	21.0	254
54	Prussian Blue Analogues for Sodiumâ€ion Batteries: Past, Present, and Future. Advanced Materials, 2022, 34, e2108384.	21.0	252

#	Article	IF	CITATIONS
55	On Similarity Preserving Feature Selection. IEEE Transactions on Knowledge and Data Engineering, 2013, 25, 619-632.	5.7	249
56	Nanostructured Si–C composite anodes for lithium-ion batteries. Electrochemistry Communications, 2004, 6, 689-692.	4.7	246
57	Nitrogenâ€Doped Graphene Ribbon Assembled Core–Sheath MnO@Graphene Scrolls as Hierarchically Ordered 3D Porous Electrodes for Fast and Durable Lithium Storage. Advanced Functional Materials, 2016, 26, 7754-7765.	14.9	245
58	Electrode reactions of manganese oxides for secondary lithium batteries. Electrochemistry Communications, 2010, 12, 1520-1523.	4.7	242
59	An investigation of polypyrrole-LiFePO4 composite cathode materials for lithium-ion batteries. Electrochimica Acta, 2005, 50, 4649-4654.	5.2	241
60	Yolk-shell silicon-mesoporous carbon anode with compact solid electrolyte interphase film for superior lithium-ion batteries. Nano Energy, 2015, 18, 133-142.	16.0	238
61	An Allâ€Integrated Anode via Interlinked Chemical Bonding between Doubleâ€Shelled–Yolkâ€Structured Silicon and Binder for Lithiumâ€Ion Batteries. Advanced Materials, 2017, 29, 1703028.	21.0	238
62	Mo ₂ C/CNT: An Efficient Catalyst for Rechargeable Li–CO ₂ Batteries. Advanced Functional Materials, 2017, 27, 1700564.	14.9	236
63	Flexible free-standing graphene-silicon composite film for lithium-ion batteries. Electrochemistry Communications, 2010, 12, 1467-1470.	4.7	234
64	Selfâ€Assembled Germanium/Carbon Nanostructures as Highâ€Power Anode Material for the Lithiumâ€lon Battery. Angewandte Chemie - International Edition, 2012, 51, 5657-5661.	13.8	231
65	Silicon/Mesoporous Carbon/Crystalline TiO ₂ Nanoparticles for Highly Stable Lithium Storage. ACS Nano, 2016, 10, 10524-10532.	14.6	230
66	General Ï€â€Electronâ€Assisted Strategy for Ir, Pt, Ru, Pd, Fe, Ni Singleâ€Atom Electrocatalysts with Bifunctional Active Sites for Highly Efficient Water Splitting. Angewandte Chemie - International Edition, 2019, 58, 11868-11873.	13.8	229
67	Anodic Oxidation Strategy toward Structure-Optimized V ₂ O ₃ Cathode <i>via</i> Electrolyte Regulation for Zn-Ion Storage. ACS Nano, 2020, 14, 7328-7337.	14.6	229
68	High-surface-area α-Fe2O3/carbon nanocomposite: one-step synthesis and its highly reversible and enhanced high-rate lithium storage properties. Journal of Materials Chemistry, 2010, 20, 2092.	6.7	228
69	Edgeâ€Hydroxylated Boron Nitride Nanosheets as an Effective Additive to Improve the Thermal Response of Hydrogels. Advanced Materials, 2015, 27, 7196-7203.	21.0	227
70	Electrochemical performance of α-Fe2O3 nanorods as anode material for lithium-ion cells. Electrochimica Acta, 2009, 54, 1733-1736.	5.2	226
71	Chemical Properties, Structural Properties, and Energy Storage Applications of Prussian Blue Analogues. Small, 2019, 15, e1900470.	10.0	226
72	Two-dimensional nanostructures for sodium-ion battery anodes. Journal of Materials Chemistry A, 2018, 6, 3284-3303.	10.3	224

#	Article	IF	CITATIONS
73	Nickel Hydroxide as an Active Material for the Positive Electrode in Rechargeable Alkaline Batteries. Journal of the Electrochemical Society, 1999, 146, 3606-3612.	2.9	223
74	Cathode materials for next generation lithium ion batteries. Nano Energy, 2013, 2, 439-442.	16.0	221
75	Ni(OH)2 Tubes with Mesoscale Dimensions as Positive-Electrode Materials of Alkaline Rechargeable Batteries. Angewandte Chemie - International Edition, 2004, 43, 4212-4216.	13.8	215
76	Ag-sheathed Bi(Pb)SrCaCuO superconducting tapes. Superconductor Science and Technology, 1993, 6, 297-314.	3.5	213
77	Sulfur–Graphene Nanostructured Cathodes <i>via</i> Ball-Milling for High-Performance Lithium–Sulfur Batteries. ACS Nano, 2014, 8, 10920-10930.	14.6	213
78	High performance MnO@C microcages with a hierarchical structure and tunable carbon shell for efficient and durable lithium storage. Journal of Materials Chemistry A, 2018, 6, 9723-9736.	10.3	212
79	Amorphous Carbon-Coated Silicon Nanocomposites:  A Low-Temperature Synthesis via Spray Pyrolysis and Their Application as High-Capacity Anodes for Lithium-Ion Batteries. Journal of Physical Chemistry C, 2007, 111, 11131-11138.	3.1	211
80	Engineering the Distribution of Carbon in Silicon Oxide Nanospheres at the Atomic Level for Highly Stable Anodes. Angewandte Chemie - International Edition, 2019, 58, 6669-6673.	13.8	209
81	Graphene wrapped LiFePO4/C composites as cathode materials for Li-ion batteries with enhanced rate capability. Journal of Materials Chemistry, 2012, 22, 16465.	6.7	206
82	High Capacity, Safety, and Enhanced Cyclability of Lithium Metal Battery Using a V ₂ O ₅ Nanomaterial Cathode and Room Temperature Ionic Liquid Electrolyte. Chemistry of Materials, 2008, 20, 7044-7051.	6.7	205
83	Critical thickness of phenolic resin-based carbon interfacial layer for improving long cycling stability of silicon nanoparticle anodes. Nano Energy, 2016, 27, 255-264.	16.0	204
84	Boosting potassium-ion batteries by few-layered composite anodes prepared via solution-triggered one-step shear exfoliation. Nature Communications, 2018, 9, 3645.	12.8	204
85	The effect of different binders on electrochemical properties of LiNi1/3Mn1/3Co1/3O2 cathode material in lithium ion batteries. Journal of Power Sources, 2013, 225, 172-178.	7.8	202
86	A Strategy for Configuration of an Integrated Flexible Sulfur Cathode for Highâ€Performance Lithium–Sulfur Batteries. Angewandte Chemie - International Edition, 2016, 55, 3992-3996.	13.8	200
87	Integrated Carbon/Red Phosphorus/Graphene Aerogel 3D Architecture via Advanced Vaporâ€Redistribution for Highâ€Energy Sodiumâ€Ion Batteries. Advanced Energy Materials, 2016, 6, 1601037.	19.5	198
88	Highâ€Performance Sodiumâ€lon Batteries and Sodiumâ€lon Pseudocapacitors Based on MoS ₂ /Graphene Composites. Chemistry - A European Journal, 2014, 20, 9607-9612.	3.3	192
89	Prelithiation: A Crucial Strategy for Boosting the Practical Application of Next-Generation Lithium Ion Battery. ACS Nano, 2021, 15, 2197-2218.	14.6	192
90	A highly ordered titania nanotube array as a supercapacitor electrode. Physical Chemistry Chemical Physics, 2011, 13, 5038.	2.8	188

#	Article	IF	CITATIONS
91	Carbon-coated MoO3 nanobelts as anode materials for lithium-ion batteries. Journal of Power Sources, 2010, 195, 2372-2376.	7.8	187
92	Hollow MnCo ₂ O ₄ Submicrospheres with Multilevel Interiors: From Mesoporous Spheres to Yolk-in-Double-Shell Structures. ACS Applied Materials & Interfaces, 2014, 6, 24-30.	8.0	187
93	A Green and Facile Way to Prepare Granadillaâ€Like Siliconâ€Based Anode Materials for Liâ€lon Batteries. Advanced Functional Materials, 2016, 26, 440-446.	14.9	187
94	Rapid microwave-assisted synthesis of Mn3O4–graphene nanocomposite and its lithium storage properties. Journal of Materials Chemistry, 2012, 22, 3600.	6.7	183
95	Investigation of cobalt oxides as anode materials for Li-ion batteries. Journal of Power Sources, 2002, 109, 142-147.	7.8	182
96	Surface Engineering and Design Strategy for Surfaceâ€Amorphized TiO ₂ @Graphene Hybrids for High Power Liâ€Ion Battery Electrodes. Advanced Science, 2015, 2, 1500027.	11.2	182
97	Free-standing single-walled carbon nanotube/SnO2 anode paper for flexible lithium-ion batteries. Carbon, 2012, 50, 1289-1297.	10.3	179
98	Studies on electrochemical behaviour of zinc-doped LiFePO4 for lithium battery positive electrode. Journal of Alloys and Compounds, 2009, 477, 498-503.	5.5	178
99	Tuning the Band Gap in Silicene by Oxidation. ACS Nano, 2014, 8, 10019-10025.	14.6	175
100	Edgeâ€Fluorinated Graphene Nanoplatelets as High Performance Electrodes for Dye‣ensitized Solar Cells and Lithium Ion Batteries. Advanced Functional Materials, 2015, 25, 1170-1179.	14.9	174
101	Study of silicon/polypyrrole composite as anode materials for Li-ion batteries. Journal of Power Sources, 2005, 146, 448-451.	7.8	172
102	Conducting Poly(aniline) Nanotubes and Nanofibers: Controlled Synthesis and Application in Lithium/Poly(aniline) Rechargeable Batteries. Chemistry - A European Journal, 2006, 12, 3082-3088.	3.3	171
103	Conductivity improvements to spray-produced LiFePO4 by addition of a carbon source. Materials Letters, 2004, 58, 1788-1791.	2.6	170
104	Large-scale synthesis of ordered mesoporous carbon fiber and its application as cathode material for lithium–sulfur batteries. Carbon, 2015, 81, 782-787.	10.3	170
105	Improved Reversibility of Fe ³⁺ /Fe ⁴⁺ Redox Couple in Sodium Super Ion Conductor Type Na ₃ Fe ₂ (PO ₄) ₃ for Sodiumâ€lon Batteries. Advanced Materials, 2017, 29, 1605694.	21.0	169
106	A Flexible 3D Multifunctional MgOâ€Decorated Carbon Foam@CNTs Hybrid as Selfâ€Supported Cathode for Highâ€Performance Lithiumâ€Sulfur Batteries. Advanced Functional Materials, 2017, 27, 1702573.	14.9	169
107	Feasibility of Cathode Surface Coating Technology for Highâ€Energy Lithiumâ€ion and Beyondâ€Lithiumâ€ion Batteries. Advanced Materials, 2017, 29, 1605807.	21.0	168
108	A new energy storage system: Rechargeable potassium-selenium battery. Nano Energy, 2017, 35, 36-43.	16.0	168

#	Article	IF	CITATIONS
109	Synthesis of tungsten disulfide (WS2) nanoflakes for lithium ion battery application. Electrochemistry Communications, 2007, 9, 119-122.	4.7	167
110	Multifunctional conducing polymer coated Na1+MnFe(CN)6 cathode for sodium-ion batteries with superior performance via a facile and one-step chemistry approach. Nano Energy, 2015, 13, 200-207.	16.0	165
111	Everlasting Living and Breathing Gyroid 3D Network in Si@SiOx/C Nanoarchitecture for Lithium Ion Battery. ACS Nano, 2019, 13, 9607-9619.	14.6	165
112	Microporous gel polymer electrolytes for lithium rechargeable battery application. Journal of Power Sources, 2012, 201, 294-300.	7.8	163
113	Facile Method To Synthesize Na-Enriched Na _{1+<i>x</i>} FeFe(CN) ₆ Frameworks as Cathode with Superior Electrochemical Performance for Sodium-Ion Batteries. Chemistry of Materials, 2015, 27, 1997-2003.	6.7	163
114	High Energy Density Sodiumâ€lon Battery with Industrially Feasible and Airâ€Stable O3â€Type Layered Oxide Cathode. Advanced Energy Materials, 2018, 8, 1701610.	19.5	161
115	Superior sodium-ion storage performance of Co ₃ O ₄ @nitrogen-doped carbon: derived from a metal–organic framework. Journal of Materials Chemistry A, 2016, 4, 5428-5435.	10.3	159
116	Cobalt phosphide as a new anode material for sodium storage. Journal of Power Sources, 2015, 294, 627-632.	7.8	158
117	Nanostructured SnSb/Carbon Nanotube Composites Synthesized by Reductive Precipitation for Lithium-Ion Batteries. Chemistry of Materials, 2007, 19, 2406-2410.	6.7	157
118	A Metalâ€Free, Freeâ€Standing, Macroporous Graphene@gâ€C ₃ N ₄ Composite Air Electrode for Highâ€Energy Lithium Oxygen Batteries. Small, 2015, 11, 2817-2824.	10.0	157
119	A new, cheap, and productive FeP anode material for sodium-ion batteries. Chemical Communications, 2015, 51, 3682-3685.	4.1	154
120	Solid Electrolyte Interphases on Sodium Metal Anodes. Advanced Functional Materials, 2020, 30, 2004891.	14.9	154
121	Electrochemical behaviour of tin borophosphate negative electrodes for energy storage systems. Journal of Power Sources, 2008, 185, 1386-1391.	7.8	153
122	Chemical bonding boosts nano-rose-like MoS2 anchored on reduced graphene oxide for superior potassium-ion storage. Nano Energy, 2019, 63, 103868.	16.0	153
123	Synthesis of vanadium pentoxide powders with enhanced surface-area for electrochemical capacitors. Journal of Power Sources, 2006, 162, 1451-1454.	7.8	152
124	Confined Fe–Cu Clusters as Subâ€Nanometer Reactors for Efficiently Regulating the Electrochemical Nitrogen Reduction Reaction. Advanced Materials, 2020, 32, e2004382.	21.0	152
125	Electrochemical lithiation and de-lithiation of MWNT–Sn/SnNi nanocomposites. Carbon, 2005, 43, 1392-1399.	10.3	151
126	Simple synthesis of yolk-shelled ZnCo2O4 microspheres towards enhancing the electrochemical performance of lithium-ion batteries in conjunction with a sodium carboxymethyl cellulose binder. Journal of Materials Chemistry A, 2013, 1, 15292.	10.3	151

#	Article	IF	CITATIONS
127	Enhanced hydrogen sorption properties of Ni and Co-catalyzed MgH2. International Journal of Hydrogen Energy, 2010, 35, 4569-4575.	7.1	149
128	SnO ₂ –Graphene Composite Synthesized via an Ultrafast and Environmentally Friendly Microwave Autoclave Method and Its Use as a Superior Anode for Lithium-Ion Batteries. Journal of Physical Chemistry C, 2011, 115, 25115-25120.	3.1	147
129	Nickel sulfide nanocrystals on nitrogen-doped porous carbon nanotubes with high-efficiency electrocatalysis for room-temperature sodium-sulfur batteries. Nature Communications, 2019, 10, 4793.	12.8	147
130	Boron-Doped Anatase TiO ₂ as a High-Performance Anode Material for Sodium-Ion Batteries. ACS Applied Materials & Interfaces, 2016, 8, 16009-16015.	8.0	145
131	Spray pyrolyzed NiO–C nanocomposite as an anode material for the lithium-ion battery with enhanced capacity retention. Solid State Ionics, 2010, 180, 1646-1651.	2.7	144
132	Novel nano-silicon/polypyrrole composites for lithium storage. Electrochemistry Communications, 2007, 9, 941-946.	4.7	141
133	Synthesis and characterization of graphene–nickel oxide nanostructures for fast charge–discharge application. Electrochimica Acta, 2011, 56, 5815-5822.	5.2	141
134	Enhancement of the electrochemical capacitance of TiO2 nanotube arrays through controlled phase transformation of anatase to rutile. Physical Chemistry Chemical Physics, 2012, 14, 4770.	2.8	138
135	Graphene-scroll-sheathed α-MnS coaxial nanocables embedded in N, S Co-doped graphene foam as 3D hierarchically ordered electrodes for enhanced lithium storage. Energy Storage Materials, 2019, 16, 46-55.	18.0	136
136	Global and Local Structure Preservation for Feature Selection. IEEE Transactions on Neural Networks and Learning Systems, 2014, 25, 1083-1095.	11.3	135
137	Investigation of discharge reaction mechanism of lithium liquid electrolyte sulfur battery. Journal of Power Sources, 2009, 189, 1179-1183.	7.8	134
138	A new class of cathode materials for rechargeable magnesium batteries: Organosulfur compounds based on sulfur–sulfur bonds. Electrochemistry Communications, 2007, 9, 1913-1917.	4.7	132
139	Spinel Li[Li1/3Ti5/3]O4 as an anode material for lithium ion batteries. Journal of Power Sources, 1999, 83, 156-161.	7.8	131
140	Electrospun P2-type Na _{2/3} (Fe _{1/2} Mn _{1/2})O ₂ Hierarchical Nanofibers as Cathode Material for Sodium-Ion Batteries. ACS Applied Materials & Interfaces, 2014, 6, 8953-8958.	8.0	131
141	Substitution-induced pinning in MgB2superconductor doped with SiC nano-particles. Superconductor Science and Technology, 2002, 15, 1587-1591.	3.5	130
142	Improving the electrochemical performance of the LiNi _{0.5} Mn _{1.5} O ₄ spinel by polypyrrole coating as a cathode material for the lithium-ion battery. Journal of Materials Chemistry A, 2015, 3, 404-411.	10.3	130
143	Large low-field magnetoresistance over a wide temperature range induced by weak-link grain boundaries in La0.7Ca0.3MnO3. Applied Physics Letters, 1998, 73, 396-398.	3.3	128
144	Silicon/Single-Walled Carbon Nanotube Composite Paper as a Flexible Anode Material for Lithium Ion Batteries. Journal of Physical Chemistry C, 2010, 114, 15862-15867.	3.1	128

#	Article	IF	CITATIONS
145	Split-half-tubular polypyrrole@sulfur@polypyrrole composite with a novel three-layer-3D structure as cathode for lithium/sulfur batteries. Nano Energy, 2015, 11, 587-599.	16.0	128
146	Nanoparticle-dispersed PEO polymer electrolytes for Li batteries. Journal of Power Sources, 2003, 119-121, 422-426.	7.8	127
147	Nanomaterials for Lithium-ion Rechargeable Batteries. Journal of Nanoscience and Nanotechnology, 2006, 6, 1-15.	0.9	127
148	Synthesis of spinel LiMn2O4 nanoparticles through one-step hydrothermal reaction. Journal of Power Sources, 2007, 172, 410-415.	7.8	127
149	MoO3 nanoparticles dispersed uniformly in carbon matrix: a high capacity composite anode for Li-ion batteries. Journal of Materials Chemistry, 2011, 21, 9350.	6.7	127
150	Structural design of anode materials for sodium-ion batteries. Journal of Materials Chemistry A, 2018, 6, 6183-6205.	10.3	127
151	A Highâ€Kinetics Sulfur Cathode with a Highly Efficient Mechanism for Superior Roomâ€īemperature Na–S Batteries. Advanced Materials, 2020, 32, e1906700.	21.0	126
152	Three-dimensional carbon frameworks enabling MoS2 as anode for dual ion batteries with superior sodium storage properties. Energy Storage Materials, 2018, 15, 22-30.	18.0	125
153	Electron Delocalization and Dissolutionâ€Restraint in Vanadium Oxide Superlattices to Boost Electrochemical Performance of Aqueous Zincâ€Ion Batteries. Advanced Energy Materials, 2020, 10, 2001852.	19.5	125
154	Rapid synthesis of α-Fe2O3/rGO nanocomposites by microwave autoclave as superior anodes for sodium-ion batteries. Journal of Power Sources, 2015, 280, 107-113.	7.8	123
155	A Comprehensive Review on Controlling Surface Composition of Ptâ€Based Bimetallic Electrocatalysts. Advanced Energy Materials, 2018, 8, 1703597.	19.5	123
156	Electrochemical Performance of Co[sub 3]O[sub 4]–C Composite Anode Materials. Electrochemical and Solid-State Letters, 2006, 9, A315.	2.2	122
157	The role of brookite in mechanical activation of anatase-to-rutile transformation of nanocrystalline TiO2: An XRD and Raman spectroscopy investigation. CrystEngComm, 2011, 13, 5055.	2.6	122
158	Bismuth sulfide: A high-capacity anode for sodium-ion batteries. Journal of Power Sources, 2016, 309, 135-140.	7.8	122
159	Porous Ni nanofibers with enhanced catalytic effect on the hydrogen storage performance of MgH ₂ . Journal of Materials Chemistry A, 2015, 3, 15843-15848.	10.3	121
160	Interplay between Electrochemistry and Phase Evolution of the P2-type Na _{<i>x</i>} (Fe _{1/2} Mn _{1/2})O ₂ Cathode for Use in Sodium-Ion Batteries. Chemistry of Materials, 2015, 27, 3150-3158.	6.7	121
161	Innovative nanosize lithium storage alloys with silica as active centre. Journal of Power Sources, 2000, 88, 278-281.	7.8	120
162	Si-based anode materials for lithium rechargeable batteries. Journal of Materials Chemistry, 2010, 20, 10055.	6.7	120

#	Article	IF	CITATIONS
163	Tin dioxide/carbon nanotube composites with high uniform SnO2 loading as anode materials for lithium ion batteries. Electrochimica Acta, 2010, 55, 2582-2586.	5.2	119
164	Construction of Structure-Tunable Si@Void@C Anode Materials for Lithium-Ion Batteries through Controlling the Growth Kinetics of Resin. ACS Nano, 2019, 13, 12219-12229.	14.6	119
165	Electrochemical deposition of porous Co3O4 nanostructured thin film for lithium-ion battery. Journal of Power Sources, 2008, 182, 359-364.	7.8	118
166	Synthesis of Co3O4/Carbon composite nanowires and their electrochemical properties. Journal of Power Sources, 2011, 196, 6987-6991.	7.8	118
167	Three dimensional cellular architecture of sulfur doped graphene: self-standing electrode for flexible supercapacitors, lithium ion and sodium ion batteries. Journal of Materials Chemistry A, 2017, 5, 5290-5302.	10.3	118
168	Commercial Prospects of Existing Cathode Materials for Sodium Ion Storage. Advanced Energy Materials, 2017, 7, 1700274.	19.5	118
169	Controlled synthesis of \hat{I}_{\pm} -Fe2O3 nanostructures and their size-dependent electrochemical properties for lithium-ion batteries. Journal of Power Sources, 2008, 184, 456-461.	7.8	117
170	Self-assembly of hierarchical star-like Co3O4 micro/nanostructures and their application in lithium ion batteries. Nanoscale, 2013, 5, 1922.	5.6	117
171	Rapid synthesis of free-standing MoO3/Graphene films by the microwave hydrothermal method as cathode for bendable lithium batteries. Journal of Power Sources, 2013, 228, 198-205.	7.8	116
172	Boosted Charge Transfer in SnS/SnO ₂ Heterostructures: Toward High Rate Capability for Sodiumâ€lon Batteries. Angewandte Chemie, 2016, 128, 3469-3474.	2.0	116
173	Potassium Nickel Iron Hexacyanoferrate as Ultra-Long-Life Cathode Material for Potassium-Ion Batteries with High Energy Density. ACS Nano, 2020, 14, 9807-9818.	14.6	116
174	Characterization of Nanocrystalline Si-MCMB Composite Anode Materials. Electrochemical and Solid-State Letters, 2004, 7, A250.	2.2	115
175	Electrochemical performance of LiFePO4 cathode material coated with ZrO2 nanolayer. Electrochemistry Communications, 2008, 10, 165-169.	4.7	114
176	A phosphorus/N-doped carbon nanofiber composite as an anode material for sodium-ion batteries. Journal of Materials Chemistry A, 2015, 3, 19011-19017.	10.3	113
177	Self-Assembled N/S Codoped Flexible Graphene Paper for High Performance Energy Storage and Oxygen Reduction Reaction. ACS Applied Materials & Interfaces, 2016, 8, 2078-2087.	8.0	113
178	Synthesis and electrochemical properties of V2O5 nanostructures prepared via a precipitation process for lithium-ion battery cathodes. Journal of Power Sources, 2007, 174, 1032-1035.	7.8	112
179	Flame spray-pyrolyzed vanadium oxide nanoparticles for lithium battery cathodes. Physical Chemistry Chemical Physics, 2009, 11, 3748.	2.8	112
180	A sequential approach to control gas for the extraction of multi-gassy coal seams from traditional gas well drainage to mining-induced stress relief. Applied Energy, 2014, 131, 67-78.	10.1	111

#	Article	IF	CITATIONS
181	A New Strategy for Achieving a High Performance Anode for Lithium Ion Batteries—Encapsulating Germanium Nanoparticles in Carbon Nanoboxes. Advanced Energy Materials, 2016, 6, 1501666.	19.5	111
182	Phosphorus and phosphide nanomaterials for sodium-ion batteries. Nano Research, 2017, 10, 4055-4081.	10.4	111
183	Mechanically strong high performance layered polypyrrole nano fibre/graphene film for flexible solid state supercapacitor. Carbon, 2014, 79, 554-562.	10.3	109
184	Atomically dispersed metal dimer species with selective catalytic activity for nitrogen electrochemical reduction. Journal of Materials Chemistry A, 2019, 7, 22242-22247.	10.3	109
185	PdNi Hollow Nanoparticles for Improved Electrocatalytic Oxygen Reduction in Alkaline Environments. ACS Applied Materials & amp; Interfaces, 2013, 5, 12708-12715.	8.0	108
186	SnSb@carbon nanocable anchored on graphene sheets for sodium ion batteries. Nano Research, 2014, 7, 1466-1476.	10.4	108
187	Effects of carbon black, graphite and carbon nanotube additives on hydrogen storage properties of magnesium. Journal of Alloys and Compounds, 2007, 427, 94-100.	5.5	107
188	Solvent-assisted molten salt process: A new route to synthesise α-Fe2O3/C nanocomposite and its electrochemical performance in lithium-ion batteries. Electrochimica Acta, 2010, 55, 5006-5013.	5.2	107
189	SnO2-coated multiwall carbon nanotube composite anode materials for rechargeable lithium-ion batteries. Electrochimica Acta, 2010, 56, 314-320.	5.2	107
190	Physical and electrochemical properties of doped lithium iron phosphate electrodes. Electrochimica Acta, 2004, 50, 443-447.	5.2	106
191	Electrochemical properties of carbon coated LiFePO4 cathode materials. Journal of Power Sources, 2005, 146, 521-524.	7.8	106
192	Carbon nanotube network modified carbon fibre paper for Li-ion batteries. Energy and Environmental Science, 2009, 2, 393.	30.8	106
193	Preparation, Characterization, and Electrochemical Performance of Li[sub 2]CuSnO[sub 4] and Li[sub 2]CuSnSiO[sub 6] Electrodes for Lithium Batteries. Journal of the Electrochemical Society, 2010, 157, A1183.	2.9	106
194	Porous AgPd–Pd Composite Nanotubes as Highly Efficient Electrocatalysts for Lithium–Oxygen Batteries. Advanced Materials, 2015, 27, 6862-6869.	21.0	106
195	Significant enhancement of the cycling performance and rate capability of the P/C composite via chemical bonding (P–C). Journal of Materials Chemistry A, 2016, 4, 505-511.	10.3	106
196	Characterization of LiM[sub x]Fe[sub 1â^'x]PO[sub 4] (M=Mg,â€,Zr,â€,Ti) Cathode Materials Prepared by the Sol-Gel Method. Electrochemical and Solid-State Letters, 2004, 7, A503.	2.2	105
197	Reversible sodium storage via conversion reaction of a MoS ₂ –C composite. Chemical Communications, 2014, 50, 10730-10733.	4.1	105
198	Free-standing sulfur-polypyrrole cathode in conjunction with polypyrrole-coated separator for flexible Li-S batteries. Energy Storage Materials, 2018, 13, 312-322.	18.0	105

#	Article	IF	CITATIONS
199	Borohydrideâ€&caffolded Li/Na/Mg Fast Ionic Conductors for Promising Solidâ€&tate Electrolytes. Advanced Materials, 2019, 31, e1803533.	21.0	105
200	Synthesis and characterization of nanosize cobalt sulfide for rechargeable lithium batteries. Journal of Power Sources, 2006, 159, 287-290.	7.8	103
201	Ultra-fine porous SnO2 nanopowder prepared via a molten salt process: a highly efficient anode material for lithium-ion batteries. Journal of Materials Chemistry, 2009, 19, 3253.	6.7	103
202	Direct synthesis of RGO/Cu2O composite films on Cu foil for supercapacitors. Journal of Alloys and Compounds, 2014, 586, 745-753.	5.5	103
203	Unique Structural Design and Strategies for Germaniumâ€Based Anode Materials Toward Enhanced Lithium Storage. Advanced Energy Materials, 2017, 7, 1700488.	19.5	103
204	Tungsten Disulfide Nanotubes for Lithium Storage. Electrochemical and Solid-State Letters, 2004, 7, A321.	2.2	102
205	Nanocrystalline NiSi alloy as an anode material for lithium-ion batteries. Journal of Alloys and Compounds, 2000, 306, 249-252.	5.5	101
206	Electrochemical properties of Si thin film prepared by pulsed laser deposition for lithium ion micro-batteries. Electrochimica Acta, 2006, 51, 5246-5249.	5.2	101
207	Synthesis of Mn3O4-anchored graphene sheet nanocomposites via a facile, fast microwave hydrothermal method and their supercapacitive behavior. Electrochimica Acta, 2013, 87, 801-808.	5.2	101
208	Electrocatalyzing S Cathodes <i>via</i> Multisulfiphilic Sites for Superior Room-Temperature Sodium–Sulfur Batteries. ACS Nano, 2020, 14, 7259-7268.	14.6	100
209	Synthesis and Characterization of LiFePO[sub 4] and LiTi[sub 0.01]Fe[sub 0.99]PO[sub 4] Cathode Materials. Journal of the Electrochemical Society, 2006, 153, A25.	2.9	99
210	Fabrication of Superior Singleâ€Atom Catalysts toward Diverse Electrochemical Reactions. Small Methods, 2019, 3, 1800497.	8.6	99
211	Atomically Thin Transitionâ€Metal Dichalcogenides for Electrocatalysis and Energy Storage. Small Methods, 2017, 1, 1700156.	8.6	98
212	Interfacial and Electronic Modulation via Localized Sulfurization for Boosting Lithium Storage Kinetics. Advanced Materials, 2020, 32, e2000151.	21.0	98
213	Enhanced Hydrogen Storage in Graphene Oxideâ€MWCNTs Composite at Room Temperature. Advanced Energy Materials, 2012, 2, 1439-1446.	19.5	97
214	Selfâ€Assembled 3D Foam‣ike NiCo ₂ O ₄ as Efficient Catalyst for Lithium Oxygen Batteries. Small, 2016, 12, 602-611.	10.0	97
215	The Quasiâ€Ptâ€Allotrope Catalyst: Hollow PtCo@singleâ€Atom Pt ₁ on Nitrogenâ€Doped Carbon toward Superior Oxygen Reduction. Advanced Functional Materials, 2019, 29, 1807340.	14.9	97
216	Synthesis and characterization of SnO2–polypyrrole composite for lithium-ion battery. Journal of Power Sources, 2007, 174, 1183-1187.	7.8	96

#	Article	IF	CITATIONS
217	Significantly improved dehydrogenation of LiBH ₄ destabilized by TiF ₃ . Energy and Environmental Science, 2010, 3, 465-470.	30.8	96
218	Boric Acid Assisted Reduction of Graphene Oxide: A Promising Material for Sodium-Ion Batteries. ACS Applied Materials & Interfaces, 2016, 8, 18860-18866.	8.0	96
219	MoO2/Mo2C/C spheres as anode materials for lithium ion batteries. Carbon, 2016, 96, 1200-1207.	10.3	96
220	Structure–Property Relationships of Organic Electrolytes and Their Effects on Li/S Battery Performance. Advanced Materials, 2017, 29, 1700449.	21.0	96
221	Few-atomic-layered hexagonal boron nitride: CVD growth, characterization, and applications. Materials Today, 2017, 20, 611-628.	14.2	96
222	Remedies for Polysulfide Dissolution in Roomâ€Temperature Sodium–Sulfur Batteries. Advanced Materials, 2020, 32, e1903952.	21.0	96
223	In Operando Mechanism Analysis on Nanocrystalline Silicon Anode Material for Reversible and Ultrafast Sodium Storage. Advanced Materials, 2017, 29, 1604708.	21.0	95
224	Ni@Pt core–shell nanoparticles with enhanced catalytic activity for oxygen reduction reaction. Journal of Alloys and Compounds, 2010, 503, L1-L4.	5.5	94
225	A high strength, free-standing cathode constructed by regulating graphitization and the pore structure in nitrogen-doped carbon nanofibers for flexible lithium–sulfur batteries. Journal of Materials Chemistry A, 2017, 5, 6832-6839.	10.3	94
226	Hydrothermal synthesis of nanostructured Co3O4 materials under pulsed magnetic field and with an aging technique, and their electrochemical performance as anode for lithium-ion battery. Electrochimica Acta, 2009, 55, 504-510.	5.2	93
227	Enhanced hydrogen storage performances of NaBH4–MgH2 system. Journal of Alloys and Compounds, 2009, 479, 619-623.	5.5	93
228	Free-standing V2O5 electrode for flexible lithium ion batteries. Electrochemistry Communications, 2011, 13, 383-386.	4.7	93
229	Nanocomposites of silicon and carbon derived from coal tar pitch: Cheap anode materials for lithium-ion batteries with long cycle life and enhanced capacity. Electrochimica Acta, 2013, 93, 213-221.	5.2	93
230	Spherical Clusters of NiO Nanoshafts for Lithium-Ion Battery Anodes. Electrochemical and Solid-State Letters, 2006, 9, A524.	2.2	92
231	Na ₃ V ₂ (PO ₄) ₃ particles partly embedded in carbon nanofibers with superb kinetics for ultra-high power sodium ion batteries. Journal of Materials Chemistry A, 2015, 3, 1005-1009.	10.3	92
232	Graphite–Tin composites as anode materials for lithium-ion batteries. Journal of Power Sources, 2001, 97-98, 211-215.	7.8	91
233	Superconductivity, critical current density, and flux pinning in MgB2â^'x(SiC)x/2 superconductor after SiC nanoparticle doping. Journal of Applied Physics, 2003, 94, 1850-1856.	2.5	91
234	Nano-structured spherical porous SnO2 anodes for lithium-ion batteries. Journal of Power Sources, 2006, 159, 345-348.	7.8	91

#	Article	IF	CITATIONS
235	Nanosize cobalt oxides as anode materials for lithium-ion batteries. Journal of Alloys and Compounds, 2002, 340, L5-L10.	5.5	90
236	Effects of CNTs on the hydrogen storage properties of MgH2 and MgH2-BCC composite. International Journal of Hydrogen Energy, 2010, 35, 7821-7826.	7.1	90
237	α-Fe2O3 as an anode material with capacity rise and high rate capability for lithium-ion batteries. Materials Research Bulletin, 2011, 46, 858-864.	5.2	90
238	Shape Evolution of α-Fe[sub 2]O[sub 3] and Its Size-Dependent Electrochemical Properties for Lithium-Ion Batteries. Journal of the Electrochemical Society, 2008, 155, A196.	2.9	89
239	Functional membrane separators for next-generation high-energy rechargeable batteries. National Science Review, 2017, 4, 917-933.	9.5	89
240	Dendriteâ€Free Sodium Metal Anodes Enabled by a Sodium Benzenedithiolateâ€Rich Protection Layer. Angewandte Chemie - International Edition, 2020, 59, 6596-6600.	13.8	89
241	Highly porous reticular tin–cobalt oxide composite thin film anodes for lithium ion batteries. Journal of Materials Chemistry, 2009, 19, 8360.	6.7	88
242	Silicon/Disordered Carbon Nanocomposites for Lithium-Ion Battery Anodes. Journal of the Electrochemical Society, 2005, 152, A2211.	2.9	86
243	Preparation of α-Fe2O3 submicro-flowers by a hydrothermal approach and their electrochemical performance in lithium-ion batteries. Electrochimica Acta, 2008, 53, 4213-4218.	5.2	86
244	Paper-like free-standing polypyrrole and polypyrrole–LiFePO4 composite films for flexible and bendable rechargeable battery. Electrochemistry Communications, 2008, 10, 1781-1784.	4.7	86
245	Interwoven V ₂ O ₅ nanowire/graphene nanoscroll hybrid assembled as efficient polysulfide-trapping-conversion interlayer for long-life lithium–sulfur batteries. Journal of Materials Chemistry A, 2018, 6, 19358-19370.	10.3	86
246	Morphology tuning of inorganic nanomaterials grown by precipitation through control of electrolytic dissociation and supersaturation. Nature Chemistry, 2019, 11, 695-701.	13.6	86
247	Targeted Synergy between Adjacent Co Atoms on Graphene Oxide as an Efficient New Electrocatalyst for Li–CO ₂ Batteries. Advanced Functional Materials, 2019, 29, 1904206.	14.9	86
248	Tailoring MXene-Based Materials for Sodium-Ion Storage: Synthesis, Mechanisms, and Applications. Electrochemical Energy Reviews, 2020, 3, 766-792.	25.5	86
249	Nano-structured SnO2-carbon composites obtained by in situ spray pyrolysis method as anodes in lithium batteries. Journal of Power Sources, 2005, 146, 180-184.	7.8	85
250	Basic molten salt process—A new route for synthesis of nanocrystalline Li4Ti5O12–TiO2 anode material for Li-ion batteries using eutectic mixture of LiNO3–LiOH–Li2O2. Journal of Power Sources, 2010, 195, 4297-4303.	7.8	85
251	Graphene–V2O5·nH2O xerogel composite cathodes for lithium ion batteries. RSC Advances, 2011, 1, 690.	3.6	84
252	Nanostructured nickel sulfide synthesized via a polyol route as a cathode material for the rechargeable lithium battery. Electrochemistry Communications, 2007, 9, 1877-1880.	4.7	83

#	Article	IF	CITATIONS
253	Improvement of electrochemical properties of the spinel LiMn2O4 using a Cr dopant effect. Solid State Ionics, 1999, 120, 95-101.	2.7	82
254	Electrochemical studies of graphitized mesocarbon microbeads as an anode in lithium-ion cells. Journal of Power Sources, 2003, 114, 292-297.	7.8	82
255	LiTi2(PO4)3 with NASICON-type structure as lithium-storage materials. Journal of Power Sources, 2003, 124, 231-236.	7.8	82
256	A Combined Hydrogen Storage System of Mg(BH ₄) ₂ â^²LiNH ₂ with Favorable Dehydrogenation. Journal of Physical Chemistry C, 2010, 114, 4733-4737.	3.1	82
257	Synthesis and electrochemical performance of doped LiCoO2 materials. Journal of Power Sources, 2007, 174, 828-831.	7.8	81
258	Mesoporous hollow PtCu nanoparticles for electrocatalytic oxygen reduction reaction. Journal of Materials Chemistry A, 2013, 1, 2391.	10.3	81
259	Multiregion Janus-Featured Cobalt Phosphide-Cobalt Composite for Highly Reversible Room-Temperature Sodium-Sulfur Batteries. ACS Nano, 2020, 14, 10284-10293.	14.6	81
260	Improvement of flux pinning in the Agâ€clad Biâ€Pbâ€5râ€Caâ€Cuâ€O wires through the use of a short period m processing. Applied Physics Letters, 1992, 60, 2929-2931.	nelt 3.3	80
261	Intergranular and intragranular critical currents in silver-sheathed Pb-Bi-Sr-Ca-Cu-O tapes. Physical Review B, 1994, 50, 10218-10224.	3.2	80
262	Al-based anode materials for Li-ion batteries. Journal of Power Sources, 2003, 119-121, 84-87.	7.8	80
263	A facile route to carbon-coated SnO2 nanoparticles combined with a new binder for enhanced cyclability of Li-ion rechargeable batteries. Electrochimica Acta, 2009, 54, 7519-7524.	5.2	80
264	Multiwalled carbon nanotube-supported Pt/Sn and Pt/Sn/PMo12 electrocatalysts for methanol electro-oxidation. International Journal of Hydrogen Energy, 2009, 34, 2426-2434.	7.1	80
265	SnO2 nanocrystals on self-organized TiO2 nanotube array as three-dimensional electrode for lithium ion microbatteries. Journal of Materials Chemistry, 2010, 20, 5689.	6.7	80
266	SnO2–NiO–C nanocomposite as a high capacity anode material for lithium-ion batteries. Journal of Materials Chemistry, 2010, 20, 9707.	6.7	80
267	A unique sandwich-structured C/Ge/graphene nanocomposite as an anode material for high power lithium ion batteries. Journal of Materials Chemistry A, 2013, 1, 14115.	10.3	80
268	A novel type of one-dimensional organic selenium-containing fiber with superior performance for lithium–selenium and sodium–selenium batteries. RSC Advances, 2014, 4, 61673-61678.	3.6	80
269	General Synthesis of Singleâ€Atom Catalysts for Hydrogen Evolution Reactions and Roomâ€Temperature Naâ€S Batteries. Angewandte Chemie - International Edition, 2020, 59, 22171-22178.	13.8	80
270	Calculation of the hysteretic force between a superconductor and a magnet. Physical Review B, 2002, 66, .	3.2	79

#	Article	IF	CITATIONS
271	Ionic conductivity and electrochemical stability of poly(methylmethacrylate)–poly(ethylene oxide) blend-ceramic fillers composites. Journal of Physics and Chemistry of Solids, 2008, 69, 243-248.	4.0	79
272	NiCo[sub 2]O[sub 4]/C Nanocomposite as a Highly Reversible Anode Material for Lithium-Ion Batteries. Electrochemical and Solid-State Letters, 2008, 11, A64.	2.2	79
273	Si-containing precursors for Si-based anode materials of Li-ion batteries: A review. Energy Storage Materials, 2016, 4, 92-102.	18.0	79
274	Growth of Highly Nitrogen-Doped Amorphous Carbon for Lithium-ion Battery Anode. Electrochimica Acta, 2016, 188, 414-420.	5.2	79
275	Design strategies for developing non-precious metal based bi-functional catalysts for alkaline electrolyte based zinc–air batteries. Materials Horizons, 2019, 6, 1812-1827.	12.2	79
276	Three-Dimensional Porous Cobalt Phosphide Nanocubes Encapsulated in a Graphene Aerogel as an Advanced Anode with High Coulombic Efficiency for High-Energy Lithium-Ion Batteries. ACS Applied Materials & Interfaces, 2019, 11, 5373-5379.	8.0	78
277	A Cation and Anion Dual Doping Strategy for the Elevation of Titanium Redox Potential for Highâ€Power Sodiumâ€Ion Batteries. Angewandte Chemie - International Edition, 2020, 59, 12076-12083.	13.8	78
278	A study on LiFePO4 and its doped derivatives as cathode materials for lithium-ion batteries. Journal of Power Sources, 2006, 159, 282-286.	7.8	77
279	β-Bi2O3 and Er3+ doped β-Bi2O3 single crystalline nanosheets with exposed reactive {001} facets and enhanced photocatalytic performance. Applied Catalysis B: Environmental, 2013, 140-141, 141-150.	20.2	77
280	Rapid synthesis of Li4Ti5O12/graphene composite with superior rate capability by a microwave-assisted hydrothermal method. Nano Energy, 2014, 8, 297-304.	16.0	77
281	Niobium doped anatase TiO ₂ as an effective anode material for sodium-ion batteries. Journal of Materials Chemistry A, 2015, 3, 22969-22974.	10.3	77
282	Boron doping-induced interconnected assembly approach for mesoporous silicon oxycarbide architecture. National Science Review, 2021, 8, nwaa152.	9.5	77
283	Electrical application of high T/sub c/ superconducting saturable magnetic core fault current limiter. IEEE Transactions on Applied Superconductivity, 1997, 7, 1009-1012.	1.7	76
284	Facile Synthesis of Hierarchical Networks Composed of Highly Interconnected V ₂ O ₅ Nanosheets Assembled on Carbon Nanotubes and Their Superior Lithium Storage Properties. ACS Applied Materials & Interfaces, 2013, 5, 12394-12399.	8.0	75
285	Enhancing the High Rate Capability and Cycling Stability of LiMn ₂ O ₄ by Coating of Solid-State Electrolyte LiNbO ₃ . ACS Applied Materials & Interfaces, 2014, 6, 22155-22165.	8.0	75
286	Hollow carbon spheres with encapsulated germanium as an anode material for lithium ion batteries. Journal of Materials Chemistry A, 2015, 3, 978-981.	10.3	75
287	Uniform Ni-rich LiNi0.6Co0.2Mn0.2O2 Porous Microspheres: Facile Designed Synthesis and Their Improved Electrochemical Performance. Electrochimica Acta, 2016, 191, 401-410.	5.2	75
288	Ultra-light and flexible pencil-trace anode for high performance potassium-ion and lithium-ion batteries. Green Energy and Environment, 2017, 2, 278-284.	8.7	75

#	Article	IF	CITATIONS
289	Core–Shell C@Sb Nanoparticles as a Nucleation Layer for High-Performance Sodium Metal Anodes. Nano Letters, 2020, 20, 4464-4471.	9.1	75
290	Hydrogen De-/Absorption Improvement of NaBH4 Catalyzed by Titanium-Based Additives. Journal of Physical Chemistry C, 2012, 116, 1596-1604.	3.1	74
291	Reverse Microemulsion Synthesis of Sulfur/Graphene Composite for Lithium/Sulfur Batteries. ACS Nano, 2017, 11, 9048-9056.	14.6	73
292	Self-assembled graphene and LiFePO4 composites with superior high rate capability for lithium ion batteries. Journal of Materials Chemistry A, 2014, 2, 4927.	10.3	72
293	Strong affinity of polysulfide intermediates to multi-functional binder for practical application in lithium–sulfur batteries. Nano Energy, 2016, 26, 722-728.	16.0	72
294	Preparation and characterization of carbon nanotubes for energy storage. Journal of Power Sources, 2003, 119-121, 16-23.	7.8	71
295	Nickel sulfide cathode in combination with an ionic liquid-based electrolyte for rechargeable lithium batteries. Solid State Ionics, 2008, 179, 2379-2382.	2.7	71
296	TiO2(B)@carbon composite nanowires as anode for lithium ion batteries with enhanced reversible capacity and cyclic performance. Journal of Materials Chemistry, 2011, 21, 8591.	6.7	71
297	A 3D porous nitrogen-doped carbon-nanofiber-supported palladium composite as an efficient catalytic cathode for lithium–oxygen batteries. Journal of Materials Chemistry A, 2017, 5, 1462-1471.	10.3	71
298	Ultrathin and Edge-Enriched Holey Nitride Nanosheets as Bifunctional Electrocatalysts for the Oxygen and Hydrogen Evolution Reactions. ACS Catalysis, 2018, 8, 9686-9696.	11.2	71
299	Synthesis and characterization of LiCoxMnyNi1â^'xâ^'yO2 as a cathode material for secondary lithium batteries. Journal of Power Sources, 2003, 119-121, 184-188.	7.8	70
300	Effects of iron oxide (Fe2O3, Fe3O4) on hydrogen storage properties of Mg-based composites. Journal of Alloys and Compounds, 2006, 422, 299-304.	5.5	70
301	Characteristics of magnesium-based hydrogen-storage alloy electrodes. Journal of Power Sources, 1995, 55, 263-267.	7.8	69
302	Effects of yttrium additions on the electrode performance of magnesium-based hydrogen storage alloys. Journal of Alloys and Compounds, 1996, 233, 236-240.	5.5	69
303	Properties of superconducting MgB2wires:in situversusex situreaction technique. Superconductor Science and Technology, 2003, 16, 639-644.	3.5	69
304	Globular reduced graphene oxide-metal oxide structures for energy storage applications. Energy and Environmental Science, 2012, 5, 5236-5240.	30.8	69
305	In situ one-step synthesis of a 3D nanostructured germanium–graphene composite and its application in lithium-ion batteries. Journal of Materials Chemistry A, 2013, 1, 10798.	10.3	69
306	Electrospinning of crystalline MoO ₃ @C nanofibers for high-rate lithium storage. Journal of Materials Chemistry A, 2015, 3, 3257-3260.	10.3	69

#	Article	IF	CITATIONS
307	Free-standing composite hydrogel films for superior volumetric capacitance. Journal of Materials Chemistry A, 2015, 3, 15668-15674.	10.3	69
308	Controllable synthesis of RGO/Fe _x O _y nanocomposites as high-performance anode materials for lithium ion batteries. Journal of Materials Chemistry A, 2014, 2, 9844-9850.	10.3	68
309	Nanoarrays: design, preparation and supercapacitor applications. RSC Advances, 2015, 5, 55856-55869.	3.6	68
310	Germanium Nanograin Decoration on Carbon Shell: Boosting Lithium‣torage Properties of Silicon Nanoparticles. Advanced Functional Materials, 2016, 26, 7800-7806.	14.9	68
311	Ice-Assisted Synthesis of Highly Crystallized Prussian Blue Analogues for All-Climate and Long-Calendar-Life Sodium Ion Batteries. Nano Letters, 2022, 22, 1302-1310.	9.1	68
312	Microstructure and defects in Ag-clad Bi-Pb-Sr-Ca-Cu-O wires prepared through a controlled melt process. Superconductor Science and Technology, 1992, 5, 591-598.	3.5	67
313	Secondary aqueous lithium-ion batteries with spinel anodes and cathodes. Journal of Power Sources, 1998, 74, 198-201.	7.8	67
314	Constructing the best symmetric full K-ion battery with the NASICON-type K3V2(PO4)3. Nano Energy, 2019, 60, 432-439.	16.0	67
315	Stress Distortion Restraint to Boost the Sodium Ion Storage Performance of a Novel Binary Hexacyanoferrate. Advanced Energy Materials, 2020, 10, 1903006.	19.5	67
316	An in-depth insight of a highly reversible and dendrite-free Zn metal anode in an hybrid electrolyte. Journal of Materials Chemistry A, 2021, 9, 4253-4261.	10.3	67
317	An investigation of polypyrrole–LiV3O8 composite cathode materials for lithium-ion batteries. Journal of Power Sources, 2007, 174, 1095-1099.	7.8	66
318	Synthesis of spherical porous vanadium pentoxide and its electrochemical properties. Journal of Power Sources, 2008, 184, 485-488.	7.8	66
319	Synthesis of hollow GeO2 nanostructures, transformation into Ge@C, and lithium storage properties. Journal of Materials Chemistry A, 2013, 1, 7666.	10.3	66
320	Carbon oated Li ₃ N Nanofibers for Advanced Hydrogen Storage. Advanced Materials, 2013, 25, 6238-6244.	21.0	66
321	Tunable Electrocatalytic Behavior of Sodiated MoS ₂ Active Sites toward Efficient Sulfur Redox Reactions in Roomâ€Temperature Na–S Batteries. Advanced Materials, 2021, 33, e2100229.	21.0	66
322	Effect of Eliminating Water in Prussian Blue Cathode for Sodiumâ€lon Batteries. Advanced Functional Materials, 2022, 32, .	14.9	66
323	Hydrogen storage properties of MgH2–SiC composites. Materials Chemistry and Physics, 2009, 114, 168-172.	4.0	65
324	Synthesis of uniform polycrystalline tin dioxide nanofibers and electrochemical application in lithium-ion batteries. Electrochimica Acta, 2010, 55, 5485-5491.	5.2	65

#	Article	IF	CITATIONS
325	Enhanced lithium storage in a VO2(B)-multiwall carbon nanotube microsheet composite prepared via an in situ hydrothermal process. Electrochimica Acta, 2010, 56, 693-699.	5.2	65
326	Rapid synthesis of binary α-NiS–β-NiS by microwave autoclave for rechargeable lithium batteries. Electrochimica Acta, 2011, 58, 456-462.	5.2	65
327	Electrospun lithium metal oxide cathode materials for lithium-ion batteries. RSC Advances, 2013, 3, 25576.	3.6	65
328	One-Step Synthesis of Graphene/Polypyrrole Nanofiber Composites as Cathode Material for a Biocompatible Zinc/Polymer Battery. ACS Applied Materials & Interfaces, 2014, 6, 16679-16686.	8.0	65
329	In Situ Grown S Nanosheets on Cu Foam: An Ultrahigh Electroactive Cathode for Room-Temperature Na–S Batteries. ACS Applied Materials & Interfaces, 2017, 9, 24446-24450.	8.0	65
330	Self-Assembling Hollow Carbon Nanobeads into Double-Shell Microspheres as a Hierarchical Sulfur Host for Sustainable Room-Temperature Sodium–Sulfur Batteries. ACS Applied Materials & Interfaces, 2018, 10, 20422-20428.	8.0	65
331	Electrochemical Deposition of Porous Co(OH)[sub 2] Nanoflake Films on Stainless Steel Mesh for Flexible Supercapacitors. Journal of the Electrochemical Society, 2008, 155, A926.	2.9	64
332	Nanoconfinement of lithium borohydride in Cu-MOFs towards low temperature dehydrogenation. Dalton Transactions, 2011, 40, 5673.	3.3	64
333	Symmetric Electrodes for Electrochemical Energyâ€Storage Devices. Advanced Science, 2016, 3, 1600115.	11.2	64
334	Equilibrium Phase Diagrams in the Systems PbO-Ag and CuO-Ag. Journal of the American Ceramic Society, 1993, 76, 2663-2664.	3.8	63
335	Synthesis and characterization of LiNiO2 compounds as cathodes for rechargeable lithium batteries. Journal of Power Sources, 1998, 76, 141-146.	7.8	63
336	In-situ hydrothermal synthesis of graphene woven VO2 nanoribbons with improved cycling performance. Journal of Power Sources, 2013, 244, 684-689.	7.8	63
337	Novel Germanium/Polypyrrole Composite for High Power Lithium-ion Batteries. Scientific Reports, 2014, 4, 6095.	3.3	63
338	Synthesis of Large and Few Atomic Layers of Hexagonal Boron Nitride on Melted Copper. Scientific Reports, 2015, 5, 7743.	3.3	63
339	Atomically Thin Hexagonal Boron Nitride Nanofilm for Cu Protection: The Importance of Film Perfection. Advanced Materials, 2017, 29, 1603937.	21.0	63
340	Low-Temperature Synthesis of Polypyrrole-Coated LiV[sub 3]O[sub 8] Composite with Enhanced Electrochemical Properties. Journal of the Electrochemical Society, 2007, 154, A633.	2.9	62
341	Effects of SiC nanoparticles with and without Ni on the hydrogen storage properties of MgH2. International Journal of Hydrogen Energy, 2009, 34, 7263-7268.	7.1	62
342	Tin/polypyrrole composite anode using sodium carboxymethyl cellulose binder for lithium-ion batteries. Dalton Transactions, 2011, 40, 12801.	3.3	62

#	Article	IF	CITATIONS
343	General Synthesis of Singleâ€Atom Catalysts for Hydrogen Evolution Reactions and Roomâ€Temperature Naâ€S Batteries. Angewandte Chemie, 2020, 132, 22355-22362.	2.0	62
344	Understanding rhombohedral iron hexacyanoferrate with three different sodium positions for high power and long stability sodium-ion battery. Energy Storage Materials, 2020, 30, 42-51.	18.0	62
345	Nanocrystalline porous α-LiFeO ₂ –C composite—an environmentally friendly cathode for the lithium-ion battery. Energy and Environmental Science, 2011, 4, 952-957.	30.8	61
346	A facile route to synthesize transition metal oxide/reduced graphene oxide composites and their lithium storage performance. RSC Advances, 2013, 3, 16597.	3.6	61
347	Sodium-difluoro(oxalato)borate (NaDFOB): a new electrolyte salt for Na-ion batteries. Chemical Communications, 2015, 51, 9809-9812.	4.1	61
348	General Synthesis of Transition Metal Oxide Ultrafine Nanoparticles Embedded in Hierarchically Porous Carbon Nanofibers as Advanced Electrodes for Lithium Storage. Advanced Functional Materials, 2016, 26, 6188-6196.	14.9	61
349	Chevrel Phase Mo ₆ T ₈ (T = S, Se) as Electrodes for Advanced Energy Storage. Small, 2017, 13, 1701441.	10.0	61
350	On the new phase (Bi,Pb)3Sr2Ca2CuOyin the Bi-Pb-Sr-Ca-Cu-O system. Superconductor Science and Technology, 1991, 4, 203-206.	3.5	60
351	Lithium storage properties of nanocrystalline eta-Cu6Sn5 alloys prepared by ball-milling. Journal of Alloys and Compounds, 2000, 299, L12-L15.	5.5	60
352	The effect of transition metals on hydrogen migration and catalysis in cast Mg–Ni alloys. International Journal of Hydrogen Energy, 2011, 36, 4984-4992.	7.1	60
353	Synthesis and electrochemical performance of LiV3O8/polyaniline as cathode material for the lithium battery. Journal of Power Sources, 2012, 220, 47-53.	7.8	60
354	Electrodeposited polypyrrole (PPy)/para (toluene sulfonic acid) (pTS) free-standing film for lithium secondary battery application. Electrochimica Acta, 2012, 60, 201-205.	5.2	60
355	Self-Assembled Multifunctional Hybrids: Toward Developing High-Performance Graphene-Based Architectures for Energy Storage Devices. ACS Central Science, 2015, 1, 206-216.	11.3	60
356	Highly Ordered Dual Porosity Mesoporous Cobalt Oxide for Sodiumâ€Ion Batteries. Advanced Materials Interfaces, 2016, 3, 1500464.	3.7	60
357	LiAlÎ Ni1â~Î O2 solid solutions as cathodic materials for rechargeable lithium batteries. Solid State Ionics, 1999, 116, 271-277.	2.7	59
358	Significant enhancement of flux pinning in MgB2 superconductor through nano-Si addition. Physica C: Superconductivity and Its Applications, 2003, 385, 461-465.	1.2	59
359	Amminelithium Amidoborane Li(NH ₃)NH ₂ BH ₃ : A New Coordination Compound with Favorable Dehydrogenation Characteristics. Chemistry - A European Journal, 2010, 16, 3763-3769.	3.3	59
360	Binderâ€Free and Carbonâ€Free 3D Porous Air Electrode for Liâ€O ₂ Batteries with High Efficiency, High Capacity, and Long Life. Small, 2016, 12, 3031-3038.	10.0	59

#	Article	IF	CITATIONS
361	Ultrathin Cobaltosic Oxide Nanosheets as an Effective Sulfur Encapsulation Matrix with Strong Affinity Toward Polysulfides. ACS Applied Materials & Interfaces, 2017, 9, 4320-4325.	8.0	59
362	An Integrated Freeâ€Standing Flexible Electrode with Holeyâ€Structured 2D Bimetallic Phosphide Nanosheets for Sodiumâ€Ion Batteries. Advanced Functional Materials, 2018, 28, 1801016.	14.9	59
363	An engineered self-supported electrocatalytic cathode and dendrite-free composite anode based on 3D double-carbon hosts for advanced Li–SeS ₂ batteries. Journal of Materials Chemistry A, 2020, 8, 2969-2983.	10.3	59
364	New approach for synthesis of carbon-mixed LiFePO4 cathode materials. Electrochimica Acta, 2004, 50, 421-426.	5.2	58
365	Spray Pyrolyzed PbO-Carbon Nanocomposites as Anode for Lithium-Ion Batteries. Journal of the Electrochemical Society, 2006, 153, A787.	2.9	58
366	Improved Hydrogen Storage of LiBH ₄ Catalyzed Magnesium. Journal of Physical Chemistry C, 2007, 111, 12495-12498.	3.1	58
367	Electrochemistry of LiV[sub 3]O[sub 8] Nanoparticles Made by Flame Spray Pyrolysis. Electrochemical and Solid-State Letters, 2008, 11, A46.	2.2	58
368	Enhanced hydrogen storage performance of LiAlH4–MgH2–TiF3 composite. International Journal of Hydrogen Energy, 2011, 36, 5369-5374.	7.1	58
369	Sodium and Lithium Storage Properties of Spray-Dried Molybdenum Disulfide-Graphene Hierarchical Microspheres. Scientific Reports, 2015, 5, 11989.	3.3	58
370	Stable Sodium Metal Anode Enabled by an Interface Protection Layer Rich in Organic Sulfide Salt. Nano Letters, 2021, 21, 619-627.	9.1	58
371	Colossal magnetoresistance in La1â^'xLixMnO3. Journal of Applied Physics, 1998, 83, 7177-7179.	2.5	57
372	Transport critical current density in Fe-sheathed nano-SiC doped MgB/sub 2/ wires. IEEE Transactions on Applied Superconductivity, 2003, 13, 3199-3202.	1.7	57
373	A Conductive Polypyrroleâ€Coated, Sulfur–Carbon Nanotube Composite for Use in Lithium–Sulfur Batteries. ChemPlusChem, 2013, 78, 318-324.	2.8	57
374	Realizing Reversible Conversionâ€Alloying of Sb(V) in Polyantimonic Acid for Fast and Durable Lithium― and Potassiumâ€Ion Storage. Advanced Energy Materials, 2020, 10, 1903119.	19.5	57
375	Mesoporous Nitrogenâ€Doped Carbon Nanospheres as Sulfur Matrix and a Novel Chelateâ€Modified Separator for Highâ€Performance Roomâ€Temperature Naâ€S Batteries. Small, 2020, 16, e1907464.	10.0	57
376	Effects of low-temperature carbon encapsulation on the electrochemical performance of SnO2 nanopowders. Carbon, 2008, 46, 35-40.	10.3	56
377	SnO2 meso-scale tubes: One-step, room temperature electrodeposition synthesis and kinetic investigation for lithium storage. Electrochemistry Communications, 2009, 11, 242-246.	4.7	56
378	Hydrogen storage properties of Mg-10Âwt% Ni alloy co-catalysed with niobium and multi-walled carbon nanotubes. International Journal of Hydrogen Energy, 2011, 36, 571-579.	7.1	56

#	Article	IF	CITATIONS
379	All-polymer battery system based on polypyrrole (PPy)/para (toluene sulfonic acid) (pTS) and polypyrrole (PPy)/indigo carmine (IC) free standing films. Electrochimica Acta, 2012, 83, 209-215.	5.2	56
380	Self-assembled porous carbon microparticles derived from halloysite clay as a lithium battery anode. Journal of Materials Chemistry A, 2017, 5, 7345-7354.	10.3	56
381	Phosphorusâ€Modulationâ€Triggered Surface Disorder in Titanium Dioxide Nanocrystals Enables Exceptional Sodiumâ€&torage Performance. Angewandte Chemie - International Edition, 2019, 58, 4022-4026.	13.8	56
382	An Emerging Energy Storage System: Advanced Na–Se Batteries. ACS Nano, 2021, 15, 5876-5903.	14.6	56
383	Flexible free-standing graphene paper with interconnected porous structure for energy storage. Journal of Materials Chemistry A, 2015, 3, 4428-4434.	10.3	55
384	Growth of MoS ₂ @C nanobowls as a lithium-ion battery anode material. RSC Advances, 2015, 5, 92506-92514.	3.6	54
385	Introducing ion-transport-regulating nanochannels to lithium-sulfur batteries. Nano Energy, 2017, 33, 205-212.	16.0	54
386	Dehydrogenation characteristics of Ti- and Ni/Ti-catalyzed Mg hydrides. Journal of Alloys and Compounds, 2009, 481, 152-155.	5.5	53
387	Study on the dehydrogenation kinetics and thermodynamics of Ca(BH4)2. Journal of Alloys and Compounds, 2010, 500, 200-205.	5.5	53
388	Facile synthesis of graphene–molybdenum dioxide and its lithium storage properties. Journal of Materials Chemistry, 2012, 22, 16072.	6.7	53
389	Influence of Ag, Cu and Fe sheaths on MgB2superconducting tapes. Superconductor Science and Technology, 2002, 15, 236-240.	3.5	52
390	A Novel Approach for Real Mass Transformation from V ₂ O ₅ Particles to Nanorods. Crystal Growth and Design, 2008, 8, 3661-3665.	3.0	52
391	Easy preparation of SnO ₂ @carbon composite nanofibers with improved lithium ion storage properties. Journal of Materials Research, 2010, 25, 1516-1524.	2.6	52
392	Layered P2â€Na _{0.66} Fe _{0.5} Mn _{0.5} O ₂ Cathode Material for Rechargeable Sodiumâ€lon Batteries. ChemElectroChem, 2014, 1, 371-374.	3.4	52
393	Highly nitrogen doped carbon nanosheets as an efficient electrocatalyst for the oxygen reduction reaction. Chemical Communications, 2015, 51, 11791-11794.	4.1	52
394	Ball-milled FeP/graphite as a low-cost anode material for the sodium-ion battery. RSC Advances, 2015, 5, 80536-80541.	3.6	52
395	Carbon-Encapsulated Sn@N-Doped Carbon Nanotubes as Anode Materials for Application in SIBs. ACS Applied Materials & amp; Interfaces, 2017, 9, 37682-37693.	8.0	52
396	Novel ionic liquid supported synthesis of platinum-based electrocatalysts on multiwalled carbon nanotubes. Electrochemistry Communications, 2006, 8, 245-250.	4.7	51

#	Article	IF	CITATIONS
397	Reversible hydrogen storage in titanium-catalyzed LiAlH4–LiBH4 system. Journal of Alloys and Compounds, 2009, 487, 434-438.	5.5	51
398	Synthesis and electrochemical performance of LiV3O8/carbon nanosheet composite as cathode material for lithium-ion batteries. Composites Science and Technology, 2011, 71, 343-349.	7.8	51
399	2D Layered Graphitic Carbon Nitride Sandwiched with Reduced Graphene Oxide as Nanoarchitectured Anode for Highly Stable Lithium-ion Battery. Electrochimica Acta, 2017, 237, 69-77.	5.2	51
400	A facile synthesis approach to micro–macroporous carbon from cotton and its application in the lithium–sulfur battery. RSC Advances, 2014, 4, 65074-65080.	3.6	50
401	A 3D hierarchical porous Co ₃ O ₄ nanotube network as an efficient cathode for rechargeable lithium–oxygen batteries. Journal of Materials Chemistry A, 2017, 5, 14673-14681.	10.3	50
402	Dendritesâ€Free Zn Metal Anodes Enabled by an Artificial Protective Layer Filled with 2D Anionic Nanosheets. Small Methods, 2021, 5, e2100650.	8.6	50
403	Stability of superconducting phases in Bi-Sr-Ca-Cu-O and the role of Pb doping. Physical Review B, 1989, 40, 5266-5269.	3.2	49
404	Electro-Oxidation of Ethanol on Pt-WO[sub 3]â^•C Electrocatalyst. Electrochemical and Solid-State Letters, 2006, 9, A423.	2.2	49
405	High capacity and high rate capability of nanostructured CuFeO2 anode materials for lithium-ion batteries. Journal of Power Sources, 2011, 196, 7025-7029.	7.8	49
406	Microwave autoclave synthesized multi-layer graphene/single-walled carbon nanotube composites for free-standing lithium-ion battery anodes. Carbon, 2014, 66, 637-645.	10.3	49
407	TiO 2 coated three-dimensional hierarchically ordered porous sulfur electrode for the lithium/sulfur rechargeable batteries. Energy, 2014, 75, 597-602.	8.8	49
408	Carbon- and binder-free 3D porous perovskite oxide air electrode for rechargeable lithium–oxygen batteries. Journal of Materials Chemistry A, 2017, 5, 5283-5289.	10.3	49
409	Progress and Challenges for Allâ€5olidâ€5tate Sodium Batteries. Advanced Energy and Sustainability Research, 2021, 2, 2000057.	5.8	49
410	Continuous Carbon Channels Enable Full Naâ€Ion Accessibility for Superior Roomâ€Temperature Na–S Batteries. Advanced Materials, 2022, 34, e2108363.	21.0	49
411	Nanostructured PbO materials obtained in situ by spray solution technique for Li-ion batteries. Journal of Power Sources, 2006, 159, 241-244.	7.8	48
412	Polyoxometallate-stabilized Pt–Ru catalysts on multiwalled carbon nanotubes: Influence of preparation conditions on the performance of direct methanol fuel cells. Journal of Power Sources, 2008, 184, 361-369.	7.8	48
413	Reversible Hydrogen Storage in Destabilized LiAlH ₄ â^'MgH ₂ â^'LiBH ₄ Ternary-Hydride System Doped with TiF ₃ . Journal of Physical Chemistry C, 2010, 114, 11643-11649.	3.1	48
414	Three-dimensional-network Li3V2(PO4)3/C composite as high rate lithium ion battery cathode material and its compatibility with ionic liquid electrolytes. Journal of Power Sources, 2014, 246, 124-131.	7.8	48

#	Article	IF	CITATIONS
415	Facile synthesis of porous V2O3/C composites as lithium storage material with enhanced capacity and good rate capability. Journal of Power Sources, 2015, 275, 392-398.	7.8	48
416	Graphiteâ€Nanoplateâ€Coated Bi ₂ S ₃ Composite with Highâ€Volume Energy Density and Excellent Cycle Life for Roomâ€Temperature Sodium–Sulfide Batteries. Chemistry - A European Journal, 2016, 22, 590-597.	3.3	48
417	A flexible 3D nitrogen-doped carbon foam@CNTs hybrid hosting TiO2 nanoparticles as free-standing electrode for ultra-long cycling lithium-ion batteries. Journal of Power Sources, 2018, 379, 10-19.	7.8	48
418	Catalytic Activity Boosting of Nickel Sulfide toward Oxygen Evolution Reaction via Confined Overdoping Engineering. ACS Applied Energy Materials, 2019, 2, 5363-5372.	5.1	48
419	Enhanced Potassium Ion Battery by Inducing Interlayer Anionic Ligands in MoS _{1.5} Se _{0.5} Nanosheets with Exploration of the Mechanism. Advanced Energy Materials, 2020, 10, 1904162.	19.5	48
420	A hybrid gel–solid-state polymer electrolyte for long-life lithium oxygen batteries. Chemical Communications, 2015, 51, 8269-8272.	4.1	47
421	Lyophilized 3D Lithium Vanadium Phosphate/Reduced Graphene Oxide Electrodes for Super Stable Lithium Ion Batteries. Advanced Energy Materials, 2016, 6, 1501760.	19.5	47
422	Bio-Derived Hierarchical Multicore–Shell Fe2N-Nanoparticle-Impregnated N-Doped Carbon Nanofiber Bundles: A Host Material for Lithium-/Potassium-Ion Storage. Nano-Micro Letters, 2019, 11, 56.	27.0	47
423	2D Titania–Carbon Superlattices Vertically Encapsulated in 3D Hollow Carbon Nanospheres Embedded with 0D TiO ₂ Quantum Dots for Exceptional Sodiumâ€lon Storage. Angewandte Chemie - International Edition, 2019, 58, 14125-14128.	13.8	47
424	Super Kinetically Pseudocapacitive MnCo ₂ S ₄ Nanourchins toward Highâ€Rate and Highly Stable Sodiumâ€Ion Storage. Advanced Functional Materials, 2020, 30, 1909702.	14.9	47
425	Recent Progress on Feâ€Based Single/Dualâ€Atom Catalysts for Zn–Air Batteries. Small, 2022, 18, e2106635.	10.0	47
426	Superconductivity in a Agâ€doped Biâ€₽bâ€&râ€Caâ€Cuâ€O system. Applied Physics Letters, 1990, 56, 493-494.	3.3	46
427	Plum-branch-like carbon nanofibers decorated with SnO2 nanocrystals. Nanoscale, 2010, 2, 1011.	5.6	46
428	Effects of Carbon Content on the Electrochemical Performances of MoS ₂ –C Nanocomposites for Li-Ion Batteries. ACS Applied Materials & Interfaces, 2016, 8, 22168-22174.	8.0	46
429	Three-Dimensional Array of TiN@Pt ₃ Cu Nanowires as an Efficient Porous Electrode for the Lithium–Oxygen Battery. ACS Nano, 2017, 11, 1747-1754.	14.6	46
430	Review of Electrolytes in Nonaqueous Lithium–Oxygen Batteries. Advanced Sustainable Systems, 2018, 2, 1700183.	5.3	46
431	Architecting Freestanding Sulfur Cathodes for Superior Roomâ€∓emperature Na–S Batteries. Advanced Functional Materials, 2021, 31, 2102280.	14.9	46
432	Electrochemical performance of SnSb and Sn/SnSb nanosize powders as anode materials in Li-ion cells. Journal of Alloys and Compounds, 2005, 400, 234-238.	5.5	45

#	Article	IF	CITATIONS
433	Characterisation of olivine-type LiMnxFe1â^'xPO4 cathode materials. Journal of Alloys and Compounds, 2006, 425, 362-366.	5.5	45
434	Liquid Crystalline Graphene Oxide/PEDOT:PSS Self-Assembled 3D Architecture for Binder-Free Supercapacitor Electrodes. Frontiers in Energy Research, 2014, 2, .	2.3	45
435	A methodical approach for fabrication of binder-free Li2S-C composite cathode with high loading of active material for Li-S battery. Carbon, 2016, 103, 163-171.	10.3	45
436	One-step synthesis of a silicon/hematite@carbon hybrid nanosheet/silicon sandwich-like composite as an anode material for Li-ion batteries. Journal of Materials Chemistry A, 2016, 4, 4056-4061.	10.3	45
437	Si–Cu/carbon composites with a core–shell structure for Li-ion secondary battery. Carbon, 2007, 45, 1928-1933.	10.3	44
438	K0.25Mn2O4nanofiber microclusters as high power cathode materials for rechargeable lithium batteries. RSC Advances, 2012, 2, 1643-1649.	3.6	44
439	Impact of mechanical bending on the electrochemical performance of bendable lithium batteries with paper-like free-standing V2O5–polypyrrole cathodes. Journal of Materials Chemistry, 2012, 22, 11159.	6.7	44
440	Enhanced rate performance of cobalt oxide/nitrogen doped graphene composite for lithium ion batteries. RSC Advances, 2013, 3, 5003.	3.6	44
441	Amorphous carbon layer contributing Li storage capacity to Nb ₂ O ₅ @C nanosheets. RSC Advances, 2015, 5, 36104-36107.	3.6	44
442	Hierarchical MnO2/rGO hybrid nanosheets as an efficient electrocatalyst for the oxygen reduction reaction. International Journal of Hydrogen Energy, 2016, 41, 5260-5268.	7.1	44
443	Investigation of Promising Air Electrode for Realizing Ultimate Lithium Oxygen Battery. Advanced Energy Materials, 2017, 7, 1700234.	19.5	44
444	Spray-pyrolyzed silicon/disordered carbon nanocomposites for lithium-ion battery anodes. Journal of Power Sources, 2007, 174, 823-827.	7.8	43
445	Electrochemical studies on LiFe1â ^{~°} xCoxPO4/carbon composite cathode materials synthesized by citrate gel technique for lithium-ion batteries. Materials Science and Engineering B: Solid-State Materials for Advanced Technology, 2008, 149, 93-98.	3.5	43
446	Submicron-sized cube-like α-Fe2O3 agglomerates as an anode material for Li-ion batteries. Electrochimica Acta, 2010, 55, 8521-8526.	5.2	43
447	Tuned In Situ Growth of Nanolayered rGO on 3D Na ₃ V ₂ (PO ₄) ₃ Matrices: A Step toward Long Lasting, High Power Naâ€ion Batteries. Advanced Materials Interfaces, 2016, 3, 1600007.	3.7	43
448	Understanding of the capacity contribution of carbon in phosphorus-carbon composites for high-performance anodes in lithium ion batteries. Nano Research, 2017, 10, 1268-1281.	10.4	43
449	Critical current density in superconducting Bi-Pb-Sr-Ca-Cu-O wires and coils. Superconductor Science and Technology, 1990, 3, 138-142.	3.5	42
450	Improvement of the LiAlH4â^'NaBH4 System for Reversible Hydrogen Storage. Journal of Physical Chemistry C, 2009, 113, 10813-10818.	3.1	42

#	Article	IF	CITATIONS
451	Durability investigation of graphene-supported Pt nanocatalysts for PEM fuel cells. Journal of Solid State Electrochemistry, 2011, 15, 1057-1062.	2.5	42
452	TiO2(B)@anatase hybrid nanowires with highly reversible electrochemical performance. Electrochemistry Communications, 2011, 13, 46-49.	4.7	42
453	Synthesis and electrochemical properties of MoO3/C nanocomposite. Electrochimica Acta, 2013, 93, 101-106.	5.2	42
454	N-Doped Crumpled Graphene Derived from Vapor Phase Deposition of PPy on Graphene Aerogel as an Efficient Oxygen Reduction Reaction Electrocatalyst. ACS Applied Materials & Interfaces, 2015, 7, 7066-7072.	8.0	42
455	Mechanism of early capacity loss of Ti2Ni hydrogen-storage alloy electrode. Journal of Power Sources, 1995, 55, 101-106.	7.8	41
456	Electrochemical characteristics of tin-coated MCMB graphite as anode in Lithium-ion cells. Electrochimica Acta, 2004, 50, 517-522.	5.2	41
457	Enhancement of Ionic Conductivity of PEO Based Polymer Electrolyte by the Addition of Nanosize Ceramic Powders. Journal of Nanoscience and Nanotechnology, 2005, 5, 1135-1140.	0.9	41
458	Thin nanostructured LiMn2O4 films by flame spray deposition and in situ annealing method. Journal of Power Sources, 2009, 189, 449-453.	7.8	41
459	Improved Hydrogen Storage Properties of NaBH ₄ Destabilized by CaH ₂ and Ca(BH ₄) ₂ . Journal of Physical Chemistry C, 2011, 115, 9283-9290.	3.1	41
460	Combined effects of hydrogen back-pressure andÂNbF5 addition on the dehydrogenation and rehydrogenation kinetics of the LiBH4–MgH2 composite system. International Journal of Hydrogen Energy, 2013, 38, 3650-3660.	7.1	41
461	Li ₂ Sâ€Based Liâ€lon Sulfur Batteries: Progress and Prospects. Small, 2021, 17, e1903934.	10.0	41
462	Processing Rusty Metals into Versatile Prussian Blue for Sustainable Energy Storage. Advanced Energy Materials, 2021, 11, 2102356.	19.5	41
463	Preparation of high T/sub c/ superconducting coils for consideration of their use in a prototype fault current limiter. IEEE Transactions on Applied Superconductivity, 1995, 5, 1051-1054.	1.7	40
464	Anisotropy of the critical current in silver sheathed (Bi,Pb)2Sr2Ca2Cu3O10tapes. Journal of Applied Physics, 1995, 78, 1123-1130.	2.5	40
465	Polyol-mediated synthesis of ultrafine tin oxide nanoparticles for reversible Li-ion storage. Electrochemistry Communications, 2007, 9, 915-919.	4.7	40
466	Highly flexible and bendable free-standing thin film polymer for battery application. Materials Letters, 2009, 63, 2352-2354.	2.6	40
467	Silver-coated TiO2 nanostructured anode materials for lithium ion batteries. Journal of Solid State Electrochemistry, 2010, 14, 571-578.	2.5	40
468	Chemical processing of double-walled carbon nanotubes for enhanced hydrogen storage. International Journal of Hydrogen Energy, 2010, 35, 6345-6349.	7.1	40

#	Article	IF	CITATIONS
469	Polypyrrole-coated α-LiFeO2 nanocomposite with enhanced electrochemical properties for lithium-ion batteries. Electrochimica Acta, 2013, 108, 820-826.	5.2	40
470	In situ engineering of urchin-like reduced graphene oxide–Mn ₂ O ₃ –Mn ₃ O ₄ nanostructures for supercapacitors. RSC Advances, 2014, 4, 886-892.	3.6	40
471	On the roles of graphene oxide doping for enhanced supercurrent in MgB ₂ based superconductors. Nanoscale, 2014, 6, 6166-6172.	5.6	40
472	Remarkable Enhancement in Sodiumâ€lon Kinetics of NaFe ₂ (CN) ₆ by Chemical Bonding with Graphene. Small Methods, 2018, 2, 1700346.	8.6	40
473	Effect of cobalt addition on the performance of titanium-based hydrogen-storage electrodes. Journal of Power Sources, 1995, 55, 197-203.	7.8	39
474	Growth of V2O5 nanorods from ball-milled powders and their performance in cathodes and anodes of lithium-ion batteries. Journal of Solid State Electrochemistry, 2010, 14, 1841-1846.	2.5	39
475	Microstructure and activation characteristics of Mg–Ni alloy modified by multi-walled carbon nanotubes. International Journal of Hydrogen Energy, 2010, 35, 4144-4153.	7.1	39
476	Improved hydrogen sorption performance of NbF5-catalysed NaAlH4. International Journal of Hydrogen Energy, 2011, 36, 14503-14511.	7.1	39
477	Nitrogen-doped carbon nanofibers with effectively encapsulated GeO ₂ nanocrystals for highly reversible lithium storage. Journal of Materials Chemistry A, 2015, 3, 21699-21705.	10.3	39
478	Mass Production and Pore Size Control of Holey Carbon Microcages. Angewandte Chemie - International Edition, 2017, 56, 13790-13794.	13.8	39
479	Few Atomic Layered Lithium Cathode Materials to Achieve Ultrahigh Rate Capability in Lithiumâ€ion Batteries. Advanced Materials, 2017, 29, 1700605.	21.0	39
480	Sustainable S cathodes with synergic electrocatalysis for room-temperature Na–S batteries. Journal of Materials Chemistry A, 2021, 9, 566-574.	10.3	39
481	Boosting electrochemical kinetics of S cathodes for room temperature Na/S batteries. Matter, 2021, 4, 1768-1800.	10.0	39
482	Rapid Formation of the 110 K Phase in BI-Pb-Sr-Ca-Cu-O through Freeze-Drying Powder Processing. Journal of the American Ceramic Society, 1990, 73, 1771-1773.	3.8	38
483	Lithium-polymer battery based on an ionic liquid–polymer electrolyte composite for room temperature applications. Electrochimica Acta, 2008, 53, 6460-6463.	5.2	38
484	Synthesis of catalyzed magnesium hydride with low absorption/desorption temperature. Scripta Materialia, 2009, 61, 469-472.	5.2	38
485	The Mechanism of the Oneâ€Step Synthesis of Hollowâ€Structured Li ₃ VO ₄ as an Anode for Lithiumâ€ion Batteries. Chemistry - A European Journal, 2014, 20, 5608-5612.	3.3	38
486	Synthesis of potential theranostic system consisting of methotrexate-immobilized (3-aminopropyl)trimethoxysilane coated α-Bi2O3 nanoparticles for cancer treatment. RSC Advances, 2014, 4, 24412.	3.6	38

#	Article	IF	CITATIONS
487	A high rate capability and long lifespan symmetric sodium-ion battery system based on a bipolar material Na ₂ LiV ₂ (PO ₄) ₃ /C. Journal of Materials Chemistry A, 2018, 6, 9962-9970.	10.3	38
488	Streamline Sulfur Redox Reactions to Achieve Efficient Roomâ€Temperature Sodium–Sulfur Batteries. Angewandte Chemie - International Edition, 2022, 61, .	13.8	38
489	Lithium insertion in Si–TiC nanocomposite materials produced by high-energy mechanical milling. Journal of Power Sources, 2005, 146, 190-194.	7.8	37
490	Mixed-metal (Li, Al) amidoborane: synthesis and enhanced hydrogen storage properties. Journal of Materials Chemistry A, 2013, 1, 1810-1820.	10.3	37
491	LiNi0.5Mn1.5O4 spinel cathode using room temperature ionic liquid as electrolyte. Electrochimica Acta, 2013, 101, 151-157.	5.2	37
492	A germanium/single-walled carbon nanotube composite paper as a free-standing anode for lithium-ion batteries. Journal of Materials Chemistry A, 2014, 2, 4613.	10.3	37
493	Effect of interfacial layers on the mechanical properties of Ag-clad Bi-based superconducting composite tapes. Superconductor Science and Technology, 1993, 6, 195-198.	3.5	36
494	Structural, physical and electrochemical characterisation of LiNixCo1â^'xO2 solid solutions. Journal of Power Sources, 2000, 85, 279-283.	7.8	36
495	Tin-based composite materials as anode materials for Li-ion batteries. Journal of Power Sources, 2003, 119-121, 45-49.	7.8	36
496	Titania nanotube supported tin anodes for lithium intercalation. Electrochemistry Communications, 2007, 9, 697-702.	4.7	36
497	Noticeable improvement in the desorption temperature from graphite in rehydrogenated MgH2/graphite composite. Materials Science & Engineering A: Structural Materials: Properties, Microstructure and Processing, 2007, 447, 180-185.	5.6	36
498	LiCoO2 cathode thin film fabricated by RF sputtering for lithium ion microbatteries. Surface and Coatings Technology, 2010, 204, 1710-1714.	4.8	36
499	Effects of polypyrrole on the performance of nickel oxide anode materials for rechargeable lithium-ion batteries. Journal of Materials Research, 2011, 26, 860-866.	2.6	36
500	Tuning three-dimensional TiO2 nanotube electrode to achieve high utilization of Ti substrate for lithium storage. Electrochimica Acta, 2014, 133, 570-577.	5.2	36
501	V 2 O 5 /Mesoporous Carbon Composite as a Cathode Material for Lithium-ion Batteries. Electrochimica Acta, 2015, 173, 172-177.	5.2	36
502	Synthesis and characterization of one-dimensional CdSe nanostructures. Applied Physics Letters, 2006, 88, 193115.	3.3	35
503	Polypyrrole as cathode materials for Zn-polymer battery with various biocompatible aqueous electrolytes. Electrochimica Acta, 2013, 95, 212-217.	5.2	35
504	Strategies Toward Stable Nonaqueous Alkali Metal–O ₂ Batteries. Advanced Energy Materials, 2019, 9, 1900464.	19.5	35

#	Article	IF	CITATIONS
505	Accelerated Polysulfide Redox in Binderâ€Free Li ₂ S Cathodes Promises Highâ€Energyâ€Density Lithium–Sulfur Batteries. Advanced Energy Materials, 2021, 11, 2100957.	19.5	35
506	Spin glass state in Gd2CoMnO6 perovskite manganite. Solid State Communications, 2001, 118, 27-30.	1.9	34
507	Preparation of orthorhombic LiMnO2 material via the sol–gel process. Journal of Power Sources, 2003, 119-121, 221-225.	7.8	34
508	An investigation on electrochemical behavior of nanosize zinc sulfide electrode in lithium-ion cells. Journal of Solid State Electrochemistry, 2006, 10, 250-254.	2.5	34
509	Stabilization of NaZn(BH ₄) ₃ via nanoconfinement in SBA-15 towards enhanced hydrogen release. Journal of Materials Chemistry A, 2013, 1, 250-257.	10.3	34
510	Mass production of three-dimensional hierarchical microfibers constructed from silicon–carbon core–shell architectures with high-performance lithium storage. Carbon, 2014, 72, 169-175.	10.3	34
511	A facile approach to synthesize stable CNTs@MnO electrocatalyst for high energy lithium oxygen batteries. Scientific Reports, 2015, 5, 8012.	3.3	34
512	3D Selenium Sulfide@Carbon Nanotube Array as Longâ€Life and Highâ€Rate Cathode Material for Lithium Storage. Advanced Functional Materials, 2018, 28, 1805018.	14.9	34
513	Synthesis of methotrexate-loaded tantalum pentoxide–poly(acrylic acid) nanoparticles for controlled drug release applications. Journal of Colloid and Interface Science, 2019, 538, 286-296.	9.4	34
514	The Emerging Electrochemical Activation Tactic for Aqueous Energy Storage: Fundamentals, Applications, and Future. Advanced Functional Materials, 2022, 32, .	14.9	34
515	A comparison of the stability of Bi2Sr2CaCu2O8+ywith YBa2Cu3O6.5+yin various solutions. Superconductor Science and Technology, 1988, 1, 194-197.	3.5	33
516	Discharge behaviour of Mg2Ni-type hydrogen-storage alloy electrodes in 6 M KOH solution by electrochemical impedance spectroscopy. Journal of Power Sources, 1996, 63, 209-214.	7.8	33
517	Preparation of Ag - Bi-2223 tape by controlling the phase evolution prior to sintering. Superconductor Science and Technology, 1996, 9, 881-887.	3.5	33
518	Improvement of critical current density in the Cu/MgB2 and Ag/MgB2 superconducting wires using the fast formation method. Physica C: Superconductivity and Its Applications, 2002, 382, 187-193.	1.2	33
519	A new rapid synthesis technique for electrochemically active materials used in energy storage applications. Electrochemistry Communications, 2006, 8, 434-438.	4.7	33
520	Polyoxometallate-stabilized platinum catalysts on multi-walled carbon nanotubes for fuel cell applications. Electrochimica Acta, 2008, 53, 6410-6416.	5.2	33
521	Preparation and Characteristics of LiFePO4 Thin Film by Radio Frequency Magnetron Sputtering for Lithium Microbatteries. Journal of Physical Chemistry C, 2009, 113, 14518-14522.	3.1	33
522	Nanofibrous Co ₃ O ₄ /PPy Hybrid with Synergistic Effect as Bifunctional Catalyst for Lithiumâ€Oxygen Batteries. Advanced Materials Interfaces, 2016, 3, 1600030.	3.7	33

#	Article	IF	CITATIONS
523	Dendriteâ€Free Sodium Metal Anodes Enabled by a Sodium Benzenedithiolateâ€Rich Protection Layer. Angewandte Chemie, 2020, 132, 6658-6662.	2.0	33
524	Recent Advances and Perspective on Electrochemical Ammonia Synthesis under Ambient Conditions. Small Methods, 2021, 5, e2100460.	8.6	33
525	Activating Inert Surface Pt Single Atoms via Subsurface Doping for Oxygen Reduction Reaction. Nano Letters, 2021, 21, 7970-7978.	9.1	33
526	Nitrogen and Oxygen Coâ€Doped Porous Hard Carbon Nanospheres with Coreâ€Shell Architecture as Anode Materials for Superior Potassiumâ€lon Storage. Small, 2022, 18, e2104296.	10.0	33
527	Superconductivity in the Bi-Pb-Sr-Ca-Cu-O system with oxide additions. Superconductor Science and Technology, 1989, 2, 274-278.	3.5	32
528	The effect of mechanical deformation on silver - core interface and critical current density in Ag - Bi-2223 single- and multifilament tapes. Superconductor Science and Technology, 1996, 9, 875-880.	3.5	32
529	Surface modification of Mg2Ni alloy in an acid solution of copper sulfate and sulfuric acid. Journal of Alloys and Compounds, 1999, 285, 267-271.	5.5	32
530	Non-aqueous synthesis of crystalline Co3O4 powders using alcohol and cobalt chloride as a versatile reaction system for controllable morphology. Journal of Power Sources, 2005, 147, 264-268.	7.8	32
531	Layered δ-MnO2 as positive electrode for lithium intercalation. Materials Letters, 2011, 65, 1319-1322.	2.6	32
532	TiO2 nanoparticles on nitrogen-doped graphene as anode material for lithium ion batteries. Journal of Nanoparticle Research, 2013, 15, 1.	1.9	32
533	The electrochemical properties of high-capacity sulfur/reduced graphene oxide with different electrolyte systems. Journal of Power Sources, 2013, 244, 240-245.	7.8	32
534	One-dimensional nanostructured design of Li _{1+x} (Mn _{1/3} Ni _{1/3} Fe _{1/3})O ₂ as a dual cathode for lithium-ion and sodium-ion batteries. Journal of Materials Chemistry A, 2015, 3, 250-257.	10.3	32
535	Engineering Highâ€Performance MoO ₂ â€Based Nanomaterials with Supercapacity and Superhydrophobicity by Tuning the Raw Materials Source. Small, 2018, 14, e1800480.	10.0	32
536	A new reflowing strategy based on lithiophilic substrates towards smooth and stable lithium metal anodes. Journal of Materials Chemistry A, 2019, 7, 18126-18134.	10.3	32
537	SnSb/Graphene Composite as Anode Materials for Lithium Ion Batteries. Advanced Science Letters, 2011, 4, 18-23.	0.2	32
538	Labile Cu3+ ions correlated with superconducting properties in YBa2Cu3O7â^'x. Solid State Communications, 1988, 68, 221-225.	1.9	31
539	Evaluation of lead—calcium—tin—aluminium grid alloys for valve-regulated lead/acid batteries. Journal of Power Sources, 1996, 59, 123-129.	7.8	31
540	Ni/Al/Co-substituted α-Ni(OH)2 as electrode materials in the nickel metal hydride cell. Journal of Alloys and Compounds, 2002, 330-332, 802-805.	5.5	31

#	Article	IF	CITATIONS
541	Electrochemical and magnetic characterization of LiFePO4 and Li0.95Mg0.05FePO4 cathode materials. Journal of Solid State Electrochemistry, 2006, 11, 177-185.	2.5	31
542	Synthesis and electrochemical properties of LiY0.1V3O8. Journal of Power Sources, 2007, 174, 548-551.	7.8	31
543	Reduction-Free Synthesis of Carbon-Encapsulated SnO ₂ Nanowires and Their Superiority in Electrochemical Performance. Journal of Physical Chemistry C, 2008, 112, 11286-11289.	3.1	31
544	Interpreting Abnormal Charge–Discharge Plateau Migration in CuxS during Long-Term Cycling. ACS Applied Materials & Interfaces, 2019, 11, 3961-3970.	8.0	31
545	Three-Dimensional Electronic Network Assisted by TiN Conductive Pillars and Chemical Adsorption to Boost the Electrochemical Performance of Red Phosphorus. ACS Nano, 2020, 14, 4609-4617.	14.6	31
546	Understanding Sulfur Redox Mechanisms in Different Electrolytes for Room-Temperature Na–S Batteries. Nano-Micro Letters, 2021, 13, 121.	27.0	31
547	Atomically dispersed S-Fe-N4 for fast kinetics sodium-sulfur batteries via a dual function mechanism. Cell Reports Physical Science, 2021, 2, 100531.	5.6	31
548	Synthesis and electrode characteristics of the new composite alloys Mg2Ni-xwt.% Ti2Ni. Journal of Alloys and Compounds, 1996, 240, 229-234.	5.5	30
549	Spin-glass state in Y0.7Ca0.3MnO3. Journal of Magnetism and Magnetic Materials, 1998, 182, L1-L4.	2.3	30
550	Electrochemical hydrogen storage properties of nonstoichiometric amorphous MgNi1+xMgNi1+x–carbon composites (x=0.05x=0.05–0.3). International Journal of Hydrogen Energy, 2006, 31, 2032-2039.	7.1	30
551	Hollow hematite nanosphere/carbon nanotube composite: mass production and its high-rate lithium storage properties. Nanotechnology, 2011, 22, 265401.	2.6	30
552	Nanoconfinement significantly improves the thermodynamics and kinetics of co-infiltrated 2LiBH4–LiAlH4 composites: Stable reversibility of hydrogen absorption/resorption. Acta Materialia, 2013, 61, 6882-6893.	7.9	30
553	Highly active Fe ₃ BO ₆ as an anode material for sodium-ion batteries. Chemical Communications, 2017, 53, 4698-4701.	4.1	30
554	A facile way to fabricate double-shell pomegranate-like porous carbon microspheres for high-performance Li-ion batteries. Journal of Materials Chemistry A, 2017, 5, 12073-12079.	10.3	30
555	Metallicâ€5tate SnS 2 Nanosheets with Expanded Lattice Spacing for Highâ€Performance Sodiumâ€ŀon Batteries. ChemSusChem, 2019, 12, 4046-4053.	6.8	30
556	Metallic state two-dimensional holey-structured Co ₃ FeN nanosheets as stable and bifunctional electrocatalysts for zinc–air batteries. Journal of Materials Chemistry A, 2019, 7, 26549-26556.	10.3	30
557	Single- and multi-filamentary Fe-sheathed MgB2 wires. Physica C: Superconductivity and Its Applications, 2002, 382, 349-354.	1.2	29
558	Optimizing synthesis of silicon/disordered carbon composites for use as anode materials in lithium-ion batteries. Journal of Power Sources, 2006, 159, 332-335.	7.8	29

#	Article	IF	CITATIONS
559	Three-dimensional Li2O–NiO–CoO composite thin-film anode with network structure for lithium-ion batteries. Journal of Power Sources, 2009, 189, 566-570.	7.8	29
560	Nanocrystalline NiO hollow spheres in conjunction with CMC for lithium-ion batteries. Journal of Applied Electrochemistry, 2010, 40, 1415-1419.	2.9	29
561	LiFePO4–Fe2P–C composite cathode: An environmentally friendly promising electrode material for lithium-ion battery. Journal of Power Sources, 2012, 206, 259-266.	7.8	29
562	Indigo carmine (IC) doped polypyrrole (PPy) as a free-standing polymer electrode for lithium secondary battery application. Solid State Ionics, 2012, 215, 29-35.	2.7	29
563	Flexible cellulose based polypyrrole–multiwalled carbon nanotube films for bio-compatible zinc batteries activated by simulated body fluids. Journal of Materials Chemistry A, 2013, 1, 14300.	10.3	29
564	Iron and nickel doped CoSe2 as efficient non precious metal catalysts for oxygen reduction. International Journal of Hydrogen Energy, 2017, 42, 236-242.	7.1	29
565	Surface Stabilization of O3-type Layered Oxide Cathode to Protect the Anode of Sodium Ion Batteries for Superior Lifespan. IScience, 2019, 19, 244-254.	4.1	29
566	Uniform Polypyrrole Layer-Coated Sulfur/Graphene Aerogel via the Vapor-Phase Deposition Technique as the Cathode Material for Li–S Batteries. ACS Applied Materials & Interfaces, 2020, 12, 5958-5967.	8.0	29
567	Alkaliâ€Metal Sulfide as Cathodes toward Safe and High apacity Metal (M = Li, Na, K) Sulfur Batteries. Advanced Energy Materials, 2020, 10, 2001764.	19.5	29
568	Electrolytes/Interphases: Enabling Distinguishable Sulfur Redox Processes in Roomâ€Temperature Sodiumâ€Sulfur Batteries. Advanced Energy Materials, 2022, 12, .	19.5	29
569	Effects of potassium-boron addition on the performance of titanium based hydrogen storage alloy electrodes. International Journal of Hydrogen Energy, 1996, 21, 373-379.	7.1	28
570	The effect of chemical coating with Ni on the electrode properties of Mg2Ni alloy. Journal of Alloys and Compounds, 1998, 280, 290-293.	5.5	28
571	Mg2Ni-based hydrogen storage alloys for metal hydride electrodes. Journal of Alloys and Compounds, 1999, 293-295, 675-679.	5.5	28
572	Nickel–cobalt oxides/carbon nanoflakes as anode materials for lithium-ion batteries. Materials Research Bulletin, 2009, 44, 140-145.	5.2	28
573	General Ï€â€Electronâ€Assisted Strategy for Ir, Pt, Ru, Pd, Fe, Ni Singleâ€Atom Electrocatalysts with Bifunctional Active Sites for Highly Efficient Water Splitting. Angewandte Chemie, 2019, 131, 11994-11999.	2.0	28
574	Bi Nanoparticles Embedded in 2D Carbon Nanosheets as an Interfacial Layer for Advanced Sodium Metal Anodes. Small, 2021, 17, e2007578.	10.0	28
575	Low-temperature surface micro-encapsulation of Ti2Ni hydrogen-storage alloy powders. Journal of Power Sources, 1994, 52, 295-299.	7.8	27
576	Effect of partial substitution of La with Ce, Pr and Nd on the properties of LaNi5-based alloy electrodes. Journal of Power Sources, 1996, 63, 267-270.	7.8	27

#	Article	IF	CITATIONS
577	Effect of the processing parameters of MgB1.8(SiC)0.1/Fe tapes on the critical current density. Physica C: Superconductivity and Its Applications, 2003, 387, 321-327.	1.2	27
578	A GBH/LiBH4 coordination system with favorable dehydrogenation. Journal of Materials Chemistry, 2011, 21, 7138.	6.7	27
579	Synthesis of nano-sized Li4Ti5O12/C composite anode material with excellent high-rate performance. Materials Letters, 2012, 68, 32-35.	2.6	27
580	Capillary-Induced Ge Uniformly Distributed in N-Doped Carbon Nanotubes with Enhanced Li-Storage Performance. Small, 2017, 13, 1700920.	10.0	27
581	Nanostructure Engineering Strategies of Cathode Materials for Room-Temperature Na–S Batteries. ACS Nano, 2022, 16, 5103-5130.	14.6	27
582	Magnetoresistance andV-lcurves of Ag-sheathed (Bi,Pb)2Sr2Ca2Cu3O10+ytape. Physical Review B, 1994, 49, 15312-15316.	3.2	26
583	Effect of sintering periods on the pinning force, activation energy and microstructure of high- superconducting Bi - (Pb) - Sr - Ca - Cu - O tapes. Superconductor Science and Technology, 1996, 9, 104-112.	3.5	26
584	Physical and electrochemical characterization of LiNi0.8Co0.2O2 thin-film electrodes deposited by laser ablation. Journal of Power Sources, 2001, 97-98, 298-302.	7.8	26
585	Synthesis of nanocrystalline transition metal and oxides for lithium storage. Journal of Power Sources, 2005, 146, 487-491.	7.8	26
586	The effects of FEC (fluoroethylene carbonate) electrolyte additive on the lithium storage properties of NiO (nickel oxide) nanocuboids. Energy, 2013, 58, 707-713.	8.8	26
587	Electrochemically active, novel layered m -ZnV 2 O 6 nanobelts for highly rechargeable Na-ion energy storage. Electrochimica Acta, 2016, 205, 62-69.	5.2	26
588	Atomic Cobalt Vacancyâ€Cluster Enabling Optimized Electronic Structure for Efficient Water Splitting. Advanced Functional Materials, 2021, 31, 2101797.	14.9	26
589	Atomic Structural Evolution of Singleâ€Layer Pt Clusters as Efficient Electrocatalysts. Small, 2021, 17, e2100732.	10.0	26
590	Recent progress on three-dimensional nanoarchitecture anode materials for lithium/sodium storage. Journal of Materials Science and Technology, 2022, 119, 167-181.	10.7	26
591	Transmission electron microscope investigation and magnetic properties of HIPed Bi-Pb-Sr-Ca-Cu-O. Superconductor Science and Technology, 1991, 4, 21-26.	3.5	25
592	Crystalline Mg2Ni obtained by mechanical alloying. Journal of Alloys and Compounds, 1996, 244, 184-189.	5.5	25
593	Studies on the diffusion coefficient of hydrogen through metal hydride electrodes. International Journal of Hydrogen Energy, 1998, 23, 177-182.	7.1	25
594	Effects of precursor powders and sintering processes on the superconducting properties of MgB2. Superconductor Science and Technology, 2004, 17, S528-S532.	3.5	25

#	Article	IF	CITATIONS
595	<i>In-Situ</i> Fabrication of Nanostructured Cobalt Oxide Powders by Spray Pyrolysis Technique. Journal of Nanoscience and Nanotechnology, 2004, 4, 861-866.	0.9	25
596	Three-dimensional reticular tin–manganese oxide composite anode materials for lithium ion batteries. Electrochimica Acta, 2010, 55, 4982-4986.	5.2	25
597	Enhanced hydrogen sorption properties in the LiBH4–MgH2 system catalysed by Ru nanoparticles supported on multiwalled carbon nanotubes. Journal of Alloys and Compounds, 2011, 509, 5012-5016.	5.5	25
598	Fast response detection of H2S by CuO-doped SnO2 films prepared by electrodeposition and oxidization at low temperature. Materials Chemistry and Physics, 2011, 130, 1325-1328.	4.0	25
599	Enhanced hydrogen storage properties of NaAlH4co-catalysed with niobium fluoride and single-walled carbon nanotubes. RSC Advances, 2012, 2, 1569-1576.	3.6	25
600	Nano-confined multi-synthesis of a Li–Mg–N–H nanocomposite towards low-temperature hydrogen storage with stable reversibility. Journal of Materials Chemistry A, 2015, 3, 12646-12652.	10.3	25
601	A systematic approach to high and stable discharge capacity for scaling up the lithium–sulfur battery. Journal of Power Sources, 2015, 279, 231-237.	7.8	25
602	Guanidinium octahydrotriborate: an ionic liquid with high hydrogen storage capacity. Journal of Materials Chemistry A, 2015, 3, 11411-11416.	10.3	25
603	<i>In situ</i> incorporation of nanostructured antimony in an N-doped carbon matrix for advanced sodium-ion batteries. Journal of Materials Chemistry A, 2019, 7, 12842-12850.	10.3	25
604	Confining Ultrathin 2D Superlattices in Mesoporous Hollow Spheres Renders Ultrafast and High apacity Naâ€Ion Storage. Advanced Energy Materials, 2020, 10, 2001033.	19.5	25
605	Efficient separators with fast Li-ion transfer and high polysulfide entrapment for superior lithium-sulfur batteries. Chemical Engineering Journal, 2021, 408, 127348.	12.7	25
606	The electrochemistry of YBa2Cu3O7–8 in aqueous potassium hydroxide. Journal of Electroanalytical Chemistry and Interfacial Electrochemistry, 1988, 248, 461-466.	0.1	24
607	Magnetic properties of a novel Prâ€Feâ€Ti phase. Journal of Applied Physics, 1994, 75, 7120-7121.	2.5	24
608	Structure and electrochemical characteristics of LiMn0.7M0.3O2 (M=Ti, V, Zn, Mo, Co, Mg, Cr). Journal of Alloys and Compounds, 2003, 348, 231-235.	5.5	24
609	Learning with multi-resolution overlapping communities. Knowledge and Information Systems, 2013, 36, 517-535.	3.2	24
610	A hybrid electrolyte energy storage device with high energy and long life using lithium anode and MnO2 nanoflake cathode. Electrochemistry Communications, 2013, 31, 35-38.	4.7	24
611	Unlocking the potential of amorphous red phosphorus films as a long-term stable negative electrode for lithium batteries. Journal of Materials Chemistry A, 2017, 5, 1925-1929.	10.3	24
612	Hierarchical Encapsulation and Rich sp ² N Assist <scp>Sb₂Se₃â€Based Conversionâ€Alloying</scp> Anode for <scp>Longâ€Life</scp> Sodium―and Potassiumâ€Ion Storage. Energy and Environmental Materials, 2023, 6, .	12.8	24

#	Article	IF	CITATIONS
613	Synthesis of Layered-Structure LiMn[sub 1â^'x]Cr[sub x]O[sub 2] by the Pechini Method and Characterization as a Cathode for Rechargeable Li/LiMnO[sub 2] Cells. Journal of the Electrochemical Society, 2002, 149, A792.	2.9	23
614	Direct visualization of iron sheath shielding effects in MgB2superconducting wires. Superconductor Science and Technology, 2003, 16, L33-L36.	3.5	23
615	The development of Y Ba2Cu3Ox thin films using a fluorine-free sol–gel approach for coated conductors. Superconductor Science and Technology, 2004, 17, 1420-1425.	3.5	23
616	Microstructure and magnetic properties in Sn1â^'xFexO2 (x=0.01, 0.05, 0.10) nanoparticles synthesized by hydrothermal method. Journal of Alloys and Compounds, 2010, 491, 679-683.	5.5	23
617	Synthesis of carbon coated nanocrystalline porous α-LiFeO2 composite and its application as anode for the lithium ion battery. Journal of Alloys and Compounds, 2011, 509, 5408-5413.	5.5	23
618	Hydrazine bisborane as a promising material for chemical hydrogen storage. International Journal of Hydrogen Energy, 2011, 36, 13640-13644.	7.1	23
619	Surface engineering of self-assembled TiO2 nanotube arrays: A practical route towards energy storage applications. Journal of Alloys and Compounds, 2014, 586, 197-201.	5.5	23
620	Exploration of the sodium ion ordered transfer mechanism in a MoSe ₂ @Graphene composite for superior rate and lifespan performance. Journal of Materials Chemistry A, 2019, 7, 13736-13742.	10.3	23
621	Heterostructured Mo2C–MoO2 as highly efficient catalyst for rechargeable Li–O2 battery. Journal of Power Sources, 2020, 470, 228317.	7.8	23
622	The Dual Functions of Defectâ€Rich Carbon Nanotubes as Both Conductive Matrix and Efficient Mediator for LiS Batteries. Small, 2021, 17, e2103535.	10.0	23
623	Novel Li ₃ VO ₄ Nanostructures Grown in Highly Efficient Microwave Irradiation Strategy and Their In‣itu Lithium Storage Mechanism. Advanced Science, 2022, 9, e2103493.	11.2	23
624	Phase evolution in silver-doped BiPbSrCaCuO(2223)/Ag superconducting composites. Journal of Materials Research, 1993, 8, 2187-2190.	2.6	22
625	Electrochemical performance of nanocrystalline lead oxide in VRLA batteries. Journal of Alloys and Compounds, 2001, 327, 141-145.	5.5	22
626	Superconductivity and flux pinning in Y and heavily Pb codoped Bi-2212 single crystals. Journal of Applied Physics, 2001, 89, 7669-7671.	2.5	22
627	Electrochemical and thermal properties of 2,4,6-tris(trifluoromethyl)-1,3,5-triazine as a flame retardant additive in Li-ion batteries. Electrochimica Acta, 2009, 54, 2259-2265.	5.2	22
628	Effects of different palladium content loading on the hydrogen storage capacity of double-walled carbon nanotubes. International Journal of Hydrogen Energy, 2012, 37, 5686-5690.	7.1	22
629	A B ₄ C nanowire and carbon nanotube composite as a novel bifunctional electrocatalyst for high energy lithium oxygen batteries. Journal of Materials Chemistry A, 2015, 3, 18395-18399.	10.3	22
630	A microwave autoclave synthesized MnO2/graphene composite as a cathode material for lithium–oxygen batteries. Journal of Applied Electrochemistry, 2016, 46, 869-878.	2.9	22

#	ARTICLE	IF	CITATIONS
631	Liquidâ€Crystalâ€Mediated Selfâ€Assembly of Porous αâ€Fe ₂ O ₃ Nanorods on PEDOT:PSSâ€Functionalized Graphene as a Flexible Ternary Architecture for Capacitive Energy Storage. Particle and Particle Systems Characterization, 2016, 33, 27-37.	2.3	22
632	Red phosphorus: A rising star of anode materials for advanced K-ion batteries. Energy Storage Materials, 2021, 42, 193-208.	18.0	22
633	Long stable cycling of fluorine-doped nickel-rich layered cathodes for lithium batteries. Sustainable Energy and Fuels, 2017, 1, 1292-1298.	4.9	22
634	Critical currents in silverâ€sheathed (Bi,Pb)2Sr2Ca2Cu3O10â^'ysuperconducting tapes. Applied Physics Letters, 1991, 59, 3171-3173.	3.3	21
635	Zinc doping effects on the structure, transport and magnetic properties of La0.7Sr0.3Mn1-xZnxO3 manganite oxide. Science and Technology of Advanced Materials, 2003, 4, 149-152.	6.1	21
636	Effect of grain size and doping level of sic on the superconductivity and critical current density in MgB/sub 2/ superconductor. IEEE Transactions on Applied Superconductivity, 2003, 13, 3273-3276.	1.7	21
637	Dehydrogenation Promotion of LiBH ₄ ·NH ₃ Through Heating in Ammonia or Mixing with Metal Hydrides. Journal of Physical Chemistry C, 2010, 114, 12823-12827.	3.1	21
638	Microwaveâ€assisted Synthesis of Flowerâ€like Structure ϵâ€MnO ₂ as Cathode for Lithium Ion Batteries. Journal of the Chinese Chemical Society, 2012, 59, 1211-1215.	1.4	21
639	Unique Urchin-like Ca2Ge7O16 Hierarchical Hollow Microspheres as Anode Material for the Lithium Ion Battery. Scientific Reports, 2015, 5, 11326.	3.3	21
640	Stable sodium metal anodes with a high utilization enabled by an interfacial layer composed of yolk–shell nanoparticles. Journal of Materials Chemistry A, 2021, 9, 13200-13208.	10.3	21
641	Labile Cu3+ions in the Bi-Sr-Ca-Cu-O system and the effects of varying the composition and heat treatment. Superconductor Science and Technology, 1988, 1, 78-82.	3.5	20
642	Studies on the performance of Ti2Ni1â^'xAlx hydrogen storage alloy electrodes. Journal of Alloys and Compounds, 1996, 233, 225-230.	5.5	20
643	On the charge/discharge behavior of Ti2Ni electrode in 6 M KOH aqueous and deuterium oxide solutions. Journal of Alloys and Compounds, 1998, 267, 224-230.	5.5	20
644	Title is missing!. Journal of Applied Electrochemistry, 1999, 29, 1-6.	2.9	20
645	Mesoporous organo-silica nanoarray for energy storage media. Electrochemistry Communications, 2007, 9, 71-75.	4.7	20
646	Allyl-substituted triazines as additives for enhancing the thermal stability of Li-ion batteries. Journal of Power Sources, 2011, 196, 1483-1487.	7.8	20
647	Liquid Crystalline Dispersions of Grapheneâ€Oxideâ€Based Hybrids: A Practical Approach towards the Next Generation of 3D Isotropic Architectures for Energy Storage Applications. Particle and Particle Systems Characterization, 2014, 31, 465-473.	2.3	20
648	A Facile Synthesis of Highâ€Surfaceâ€Area Sulfur–Carbon Composites for Li/S Batteries. Chemistry - A European Journal, 2015, 21, 10061-10069.	3.3	20

#	Article	IF	CITATIONS
649	Carbon- and crack-free growth of hexagonal boron nitride nanosheets and their uncommon stacking order. Nanoscale, 2016, 8, 15926-15933.	5.6	20
650	Energy storage in Oceania. Energy Storage Materials, 2019, 20, 176-187.	18.0	20
651	A Cation and Anion Dual Doping Strategy for the Elevation of Titanium Redox Potential for Highâ€Power Sodiumâ€lon Batteries. Angewandte Chemie, 2020, 132, 12174-12181.	2.0	20
652	Effects of carbon on electrochemical performance of red phosphorus (P) and carbon composite as anode for sodium ion batteries. Journal of Materials Science and Technology, 2021, 68, 140-146.	10.7	20
653	Facile Fabrication of Ag Nanocrystals Encapsulated in Nitrogenâ€doped Fibrous Carbon as an Efficient Catalyst for Lithium Oxygen Batteries. Energy and Environmental Materials, 2021, 4, 239-245.	12.8	20
654	Electrochemical release of catalysts in nanoreactors for solid sulfur redox reactions in room-temperature sodium-sulfur batteries. Cell Reports Physical Science, 2021, 2, 100539.	5.6	20
655	CoS ₂ Nanoparticles Anchored on MoS ₂ Nanorods As a Superior Bifunctional Electrocatalyst Boosting Li ₂ O ₂ Heteroepitaxial Growth for Rechargeable Liâ€O ₂ Batteries. Small, 2022, 18, e2105752.	10.0	20
656	Critical current density and irreversibility behaviour in Ag-sheathed Bi-based superconducting wires fabricated using a controlled melt procedure. Applied Superconductivity, 1993, 1, 1515-1522.	0.5	19
657	High voltage generation with a high T/sub c/ superconducting resonant circuit. IEEE Transactions on Applied Superconductivity, 1997, 7, 881-884.	1.7	19
658	Hydrogen desorption and electrode properties of Zr0.8Ti0.2(V0.3Ni0.6M0.1)2. Journal of Alloys and Compounds, 1997, 256, 40-44.	5.5	19
659	Phase development and kinetics of high temperature Bi-2223 phase. Journal of Alloys and Compounds, 1998, 281, 280-289.	5.5	19
660	Structure characteristics and lithium ionic conductivity of La(0.57â^2x/3)SrxLi0.3TiO3 perovskites. Journal of Materials Science, 2000, 35, 4289-4291.	3.7	19
661	Preparation and properties of spherical LiNi0.75Co0.25O2 as a cathode for lithium-ion batteries. Electrochimica Acta, 2004, 50, 435-441.	5.2	19
662	Enhancement of critical current density in YBa2Cu3O7ÂÂ thin films grown using PLD on YSZ (001) surface modified with Ag nano-dots. Journal Physics D: Applied Physics, 2004, 37, 1824-1828.	2.8	19
663	In situ fabrication of spherical porous tin oxide via a spray pyrolysis technique. Electrochimica Acta, 2006, 51, 3680-3684.	5.2	19
664	Comparison of Few-layer Graphene Prepared from Natural Graphite through Fast Synthesis Approach. Journal of Materials Science and Technology, 2015, 31, 907-912.	10.7	19
665	Sodium borohydride hydrazinates: synthesis, crystal structures, and thermal decomposition behavior. Journal of Materials Chemistry A, 2015, 3, 11269-11276.	10.3	19
666	3-D structured SnO ₂ –polypyrrole nanotubes applied in Na-ion batteries. RSC Advances, 2016, 6, 103124-103131.	3.6	19

#	Article	IF	CITATIONS
667	An improved synthesis of unsolvated NaB 3 H 8 and its application in preparing Na 2 B 12 H 12. International Journal of Hydrogen Energy, 2016, 41, 15471-15476.	7.1	19
668	A Strategy for Configuration of an Integrated Flexible Sulfur Cathode for Highâ€Performance Lithium–Sulfur Batteries. Angewandte Chemie, 2016, 128, 4060-4064.	2.0	19
669	Biocompatible Bi(OH)3 nanoparticles with reduced photocatalytic activity as possible ultraviolet filter in sunscreens. Materials Research Bulletin, 2018, 108, 130-141.	5.2	19
670	Understanding the Effects of the Low-Concentration Electrolyte on the Performance of High-Energy-Density Li–S Batteries. ACS Applied Materials & Interfaces, 2021, 13, 28405-28414.	8.0	19
671	Enhancement of critical current density in the Bi-Pb-Sr-Ca-Cu-O system by addition of Ca2CuO3. Superconductor Science and Technology, 1989, 2, 308-310.	3.5	18
672	Cu valence states in superconducting Biî—,Pbî—,Srî—,Caî—,Cuî—,O system. Journal of Solid State Chemistry, 1990, 289-297.	87 2.9	18
673	Superconducting properties of Au/Bi-Pb-Sr-Ca-Cu-O composites. Superconductor Science and Technology, 1990, 3, 210-212.	3.5	18
674	Effect of Ca2CuO3 excess on superconducting properties in the Bi–Pb–Sr–Ca–Cu–O system. Journal or Materials Research, 1991, 6, 2287-2290.	f _{2.6}	18
675	Large irreversible magnetization arising from the domain freezing in La0.7Ca0.3MnO3 perovskite. Solid State Communications, 1998, 108, 661-665.	1.9	18
676	Multiple-ion-doped lithium nickel oxides as cathode materials for lithium-ion batteries. Journal of Power Sources, 2003, 119-121, 189-194.	7.8	18
677	Improvement in hydrogen cycling properties of magnesium through added graphite. Materials Letters, 2007, 61, 3163-3166.	2.6	18
678	Improved reversible dehydrogenation of 2LiBH ₄ +MgH ₂ system by introducing Ni nanoparticles. Journal of Materials Research, 2011, 26, 1143-1150.	2.6	18
679	Core-Shell Co/CoO Integrated on 3D Nitrogen Doped Reduced Graphene Oxide Aerogel as an Enhanced Electrocatalyst for the Oxygen Reduction Reaction. Frontiers in Chemistry, 2016, 4, 36.	3.6	18
680	Highly Stable Lithium/Sodium Metal Batteries with High Utilization Enabled by a Holey Two-Dimensional N-Doped TiNb ₂ O ₇ Host. Nano Letters, 2021, 21, 10453-10461.	9.1	18
681	Conductivity and microstructure of bismuth oxide-based electrolytes with enhanced stability. Solid State Ionics, 1993, 66, 201-206.	2.7	17
682	Development of microstructure and superconductivity of silver-clad Bi(2223) composite tapes in the process of heat treatment. Materials Science and Engineering B: Solid-State Materials for Advanced Technology, 1994, 23, 58-65.	3.5	17
683	Effect of silver on the processing and properties of tapes. Applied Superconductivity, 1994, 2, 191-199.	0.5	17
684	Study on interfaces and microstructural defects in Ag-clad (Bi,Pb)2Sr2Ca2Cu3O10+ytapes. Superconductor Science and Technology, 1995, 8, 168-173.	3.5	17

#	Article	IF	CITATIONS
685	Effect of pressing and Li doping on superconducting properties of Ag-sheathed Bi-2223 tapes. Superconductor Science and Technology, 1998, 11, 1061-1064.	3.5	17
686	Effect of oxygen partial pressure on processing conditions and phase transformation in Ag/Bi-2223 tapes. Physica C: Superconductivity and Its Applications, 2001, 351, 371-378.	1.2	17
687	Study of structure, transport, paramagnetic and ferromagnetic properties of La0.8Sr0.2Mn1â^'xZnxO3perovskite manganite. Superconductor Science and Technology, 2002, 15, 346-350.	3.5	17
688	Structure and spin glass behaviour in non-metallic Yb2CoMnO6 perovskite manganite. Journal of Magnetism and Magnetic Materials, 2002, 246, 86-92.	2.3	17
689	Electrochemical properties of nanosize Sn-coated graphite anodes in lithium-ion cells. Journal of Applied Electrochemistry, 2004, 34, 187-190.	2.9	17
690	The compatibility of transition metal oxide/carbon composite anode and ionic liquid electrolyte for the lithium-ion battery. Journal of Applied Electrochemistry, 2011, 41, 1261-1267.	2.9	17
691	An overview—Functional nanomaterials for lithium rechargeable batteries, supercapacitors, hydrogen storage, and fuel cells. Materials Research Bulletin, 2013, 48, 4968-4973.	5.2	17
692	CuS Nanoflakes, Microspheres, Microflowers, and Nanowires: Synthesis and Lithium Storage Properties. Journal of Nanoscience and Nanotechnology, 2013, 13, 1309-1316.	0.9	17
693	Effects of substituting Cu for Sn on the microstructure and hydrogen absorption properties of Co-free AB5 alloys. International Journal of Hydrogen Energy, 2016, 41, 17022-17028.	7.1	17
694	Chemically Bonded Sn Nanoparticles Using the Crosslinked Epoxy Binder for High Energyâ€Density Li Ion Battery. Advanced Materials Interfaces, 2016, 3, 1600662.	3.7	17
695	High energy density of Li 3â^'x Na x V 2 (PO 4) 3 /C cathode material with high rate cycling performance for lithium-ion batteries. Journal of Power Sources, 2017, 357, 117-125.	7.8	17
696	Carbonaceous Hosts for Sulfur Cathode in Alkaliâ€Metal/S (Alkali Metal = Lithium, Sodium, Potassium) Batteries. Small, 2021, 17, e2006504.	10.0	17
697	Influence of alloying with bismuth on electrochemical behaviour of lead-calcium-tin grid alloys. Journal of Power Sources, 1997, 66, 107-113.	7.8	16
698	Effect of ball milling materials and methods on powder processing of Bi2223 superconductors. Superconductor Science and Technology, 1998, 11, 1153-1159.	3.5	16
699	Lithium Storage Properties of Ball Milled Ni-57 mass%Sn Alloy. Materials Transactions, 2002, 43, 63-66.	1.2	16
700	Improved dehydrogenation properties of the combined Mg(BH4)2•6NH3–nNH3BH3 system. International Journal of Hydrogen Energy, 2013, 38, 16199-16207.	7.1	16
701	Porous Ni0.5Zn0.5Fe2O4 Nanospheres: Synthesis, Characterization, and Application for Lithium Storage. Electrochimica Acta, 2014, 147, 143-150.	5.2	16
702	In-situ One-step Hydrothermal Synthesis of a Lead Germanate-Graphene Composite as a Novel Anode Material for Lithium-Ion Batteries. Scientific Reports, 2014, 4, 7030.	3.3	16

#	Article	IF	CITATIONS
703	Hierarchical Porous Li2Mg(NH)2@C Nanowires with Long Cycle Life Towards Stable Hydrogen Storage. Scientific Reports, 2014, 4, 6599.	3.3	16
704	Engineering the Distribution of Carbon in Silicon Oxide Nanospheres at the Atomic Level for Highly Stable Anodes. Angewandte Chemie, 2019, 131, 6741-6745.	2.0	16
705	Copper phosphide as a promising anode material for potassium-ion batteries. Journal of Materials Chemistry A, 2021, 9, 8378-8385.	10.3	16
706	Regulating the Electronic Configuration of Supported Iron Nanoparticles for Electrochemical Catalytic Nitrogen Fixation. Advanced Functional Materials, 2022, 32, .	14.9	16
707	Effect of mechanical deformation on the mass density of Ag-clad (Bi,Pb)2Sr2Ca2Cu3O10 wire and tape. Applied Superconductivity, 1996, 4, 17-24.	0.5	15
708	Fabrication and critical current density in 16-filament stainless steel/Fe/MgB2 square wire. Solid State Communications, 2002, 124, 59-62.	1.9	15
709	Pt1â^'Co nanoparticles as cathode catalyst for proton exchange membrane fuel cells with enhanced catalytic activity. Materials Chemistry and Physics, 2010, 124, 841-844.	4.0	15
710	Effect of different reductants for palladium loading on hydrogen storage capacity of double-walled carbon nanotubes. International Journal of Hydrogen Energy, 2011, 36, 9032-9036.	7.1	15
711	Pt–Ni/C catalysts using different carbon supports for the cathode of the proton exchange membrane fuel cell (PEMFC). Materials Chemistry and Physics, 2012, 136, 845-849.	4.0	15
712	Well-dispersed lithium amidoborane nanoparticles through nanoreactor engineering for improved hydrogen release. Nanoscale, 2014, 6, 12333-12339.	5.6	15
713	Ammonium Aminodiboranate: A Long‣ought Isomer of Diammoniate of Diborane and Ammonia Borane Dimer. Chemistry - A European Journal, 2016, 22, 7727-7729.	3.3	15
714	Ternary Porous Sulfur/Dual-Carbon Architectures for Lithium/Sulfur Batteries Obtained Continuously and on a Large Scale via an Industry-Oriented Spray-Pyrolysis/Sublimation Method. ACS Applied Materials & Interfaces, 2016, 8, 25251-25260.	8.0	15
715	High toxicity of Bi(OH)3 and $\hat{1}\pm$ -Bi2O3 nanoparticles towards malignant 9L and MCF-7 cells. Materials Science and Engineering C, 2018, 93, 958-967.	7.3	15
716	Improved single crystal growth in the Bi-Sr-Ca-Cu-O system using a sealed cavity technique. Journal of Crystal Growth, 1990, 100, 303-308.	1.5	14
717	Transport and magnetisation measurements of Bi2223/Ag tapes and the role of granularity on critical current limitation. IEEE Transactions on Applied Superconductivity, 1995, 5, 1391-1394.	1.7	14
718	Improvement of flux pinning by thermo-mechanical treatment of Bi-2223/Ag superconducting tapes. Superconductor Science and Technology, 1997, 10, 409-415.	3.5	14
719	Powder production methods of Bi-Pb-Sr-Ca-Cu-O superconductors. Superconductor Science and Technology, 1998, 11, 1166-1172.	3.5	14
720	Electrochemical study on orthorhombic LiMnO2 as cathode in rechargeablelithium batteries. Journal of Applied Electrochemistry, 1999, 29, 1423-1426.	2.9	14

#	Article	IF	CITATIONS
721	Mg2Ni hydride electrodes prepared by sintering and subsequent ball milling with Ni powders. Journal of Alloys and Compounds, 1999, 293-295, 536-540.	5.5	14
722	Effect of various mechanical deformation techniques on critical current densities of Ag/Bi-2223 tapes. Physica C: Superconductivity and Its Applications, 2001, 354, 349-352.	1.2	14
723	Beneficial effects of red lead on non-cured plates for lead-acid batteries. Journal of Power Sources, 2003, 113, 371-375.	7.8	14
724	Nano-sized Al2O3 doping effects on the critical current density of MgB2 superconductors. Ceramics International, 2004, 30, 1581-1583.	4.8	14
725	Preparation of spherical clusters of metal oxide nanorods and their hydrogen storage behavior. Materials Letters, 2006, 60, 3891-3894.	2.6	14
726	Studies on film formation on cathodes using pyrazole derivatives as electrolyte additives in the Li-ion battery. Electrochemistry Communications, 2009, 11, 1657-1660.	4.7	14
727	Three-dimensional nanocarbon and the electrochemistry of nanocarbon/tin oxide for lithium ion batteries. Journal of Solid State Electrochemistry, 2011, 15, 2645-2652.	2.5	14
728	A novel high voltage battery cathodes of Fe 2+ /Fe 3+ sodium fluoro sulfate lined with carbon nanotubes for stable sodium batteries. Journal of Power Sources, 2018, 398, 175-182.	7.8	14
729	Enhanced flux pinning from CuO inclusions in Bi2Sr2CaCu2Oycrystals. Journal of Applied Physics, 1997, 81, 533-535.	2.5	13
730	Formation of FeTi Hydrogen Storage Alloys by Ball-milling. Journal of Materials Science Letters, 1998, 17, 1825-1830.	0.5	13
731	Microstructural study of Bi2223/Ag tapes made using a two-stage sintering procedure. Superconductor Science and Technology, 1998, 11, 505-508.	3.5	13
732	Optimal reduction in rolling Ag-sheathed Bi-2223 multifilamentary tapes. Superconductor Science and Technology, 1998, 11, 299-303.	3.5	13
733	Characteristics of micro-texture and meso-texture in (Bi, Pb)2Sr2Ca2Cu3O10superconducting tapes. Superconductor Science and Technology, 2001, 14, 471-478.	3.5	13
734	Structure and electrochemistry of LiCrxMn1â^'xO2 cathode for lithium-ion batteries. Solid State lonics, 2002, 148, 359-366.	2.7	13
735	Start-Fine-Particle Carbon-enriched Li0.98Mg0.02FePO4 Synthesized by A Novel Modified Solid-State Reaction. Synthetic Metals, 2005, 153, 113-116.	3.9	13
736	Reversible storage of hydrogen in NaF–MB2 (M = Mg, Al) composites. Journal of Materials Chemistry A, 2013, 1, 2806.	10.3	13
737	Regeneration of alkaline metal amidoboranes with high purity. International Journal of Hydrogen Energy, 2016, 41, 407-412.	7.1	13
738	2D Titania–Carbon Superlattices Vertically Encapsulated in 3D Hollow Carbon Nanospheres Embedded with 0D TiO 2 Quantum Dots for Exceptional Sodiumâ€lon Storage. Angewandte Chemie, 2019, 131, 14263-14266.	2.0	13

#	Article	IF	CITATIONS
739	Effect of silver additions on properties of high-temperature superconducting tapes. Materials Letters, 1994, 18, 336-340.	2.6	12
740	Surface and electrode properties of Zr(V0.25Ni0.75)2 alloy treated with ultrasound-solution. Journal of Alloys and Compounds, 1998, 265, 281-285.	5.5	12
741	Critical current density significantly enhanced by hot pressing in Bi-2223/Ag multifilamentary tapes. Superconductor Science and Technology, 1998, 11, 1101-1104.	3.5	12
742	The formation and distribution of texture microstructure produced by mechanical deformation in silver-sheathed BSCCO superconductors. Superconductor Science and Technology, 1998, 11, 1011-1016.	3.5	12
743	Study of the magnetic phase transition in La0.7Ca0.3MnO3 using a magneto-optical method. Applied Physics Letters, 1999, 74, 3014-3016.	3.3	12
744	Effect of grain connectivity and density on the magnetoresistance in Ca or Li doped lanthanum manganites. Solid State Communications, 2000, 117, 53-56.	1.9	12
745	Crystal growth patterns in MgO seeded Y1.8Ba2.4Cu3.4Oy/Ag melt-texturing process. Physica C: Superconductivity and Its Applications, 2001, 357-360, 734-737.	1.2	12
746	Crystallographic orientation mapping with an electron backscattered diffraction technique in (Bi,) Tj ETQq0 0 0 r	gB <u>T</u> /Over	lock 10 Tf 50
747	Electrochemical properties of orthorhombic LiMnO2 prepared by one-step middle-temperature solid-state reaction. Journal of Alloys and Compounds, 2002, 346, 255-259.	5.5	12
748	Studies on electrochemical performance of partially reduced MnO2 used as cathode for MH–MnO2 rechargeable battery. Journal of Power Sources, 2002, 109, 11-16.	7.8	12
749	Nanostructured NiO/C Composite for Lithium-Ion Battery Anode. Journal of Nanoscience and Nanotechnology, 2009, 9, 1951-1955.	0.9	12
750	Preparation and electrochemical performance of hollow-spherical polypyrrole/V2O5 composite. Transactions of Nonferrous Metals Society of China, 2011, 21, 1303-1308.	4.2	12
751	A Hierarchical Word-Merging Algorithm with Class Separability Measure. IEEE Transactions on Pattern Analysis and Machine Intelligence, 2014, 36, 417-435.	13.9	12
752	Study on Vanadium Substitution to Iron in Li2FeP2O7 as Cathode Material for Lithium-ion Batteries. Electrochimica Acta, 2014, 141, 195-202.	5.2	12
753	A chemically modified graphene oxide wrapped porous hematite nano-architecture as a high rate lithium-ion battery anode material. RSC Advances, 2016, 6, 82698-82706.	3.6	12
754	Metal-oxygen bonds: Stabilizing the intermediate species towards practical Li-air batteries. Electrochimica Acta, 2018, 259, 313-320.	5.2	12
755	TiO ₂ /(BiO) ₂ CO ₃ nanocomposites for ultraviolet filtration with reduced photocatalytic activity. Journal of Materials Chemistry C, 2018, 6, 5639-5650.	5.5	12
756	Effect of sintering periods on the microstructure and electrical transport properties of high-Tc superconducting Bi–(Pb)–Sr–Ca–Cu–O tapes. Journal of Materials Research, 1996, 11, 1101-1107.	2.6	11

#	Article	IF	CITATIONS
757	Title is missing!. Journal of Materials Science, 1997, 32, 2629-2635.	3.7	11
758	Optimization of processing to improve critical current density of Ag/Bi-2223 tapes. Superconductor Science and Technology, 1998, 11, 915-920.	3.5	11
759	Critical role of phase transformation during processing of Ag/Bi:2223 tapes. IEEE Transactions on Applied Superconductivity, 1999, 9, 2436-2439.	1.7	11
760	Critical current degradation caused by winding process of Bi-2223/Ag HTS wire in the form of a coil. IEEE Transactions on Applied Superconductivity, 1999, 9, 138-141.	1.7	11
761	Structure characterisation and lithium insertion in La0.33NbO3 perovskite. Solid State Ionics, 1999, 124, 37-43.	2.7	11
762	Up-conversion luminescence of ytterbium and thulium codoped potassium yttrium double tungstate crystal. Crystal Research and Technology, 2002, 37, 1318-1324.	1.3	11
763	Electrochemical Hydrogen Storage in Single-Walled Carbon Nanotube Paper. Journal of Nanoscience and Nanotechnology, 2006, 6, 713-718.	0.9	11
764	Hexagonalâ€5haped Tin Glycolate Particles: A Preliminary Study of Their Suitability as Liâ€lon Insertion Electrodes. Chemistry - an Asian Journal, 2008, 3, 854-861.	3.3	11
765	Dehydrogenation/rehydrogenation mechanism in aluminum destabilized lithium borohydride. Journal of Materials Research, 2009, 24, 2720-2727.	2.6	11
766	Application of statistical methodology for the evaluation of mechanically activated phase transformation in nanocrystalline TiO2. Journal of Alloys and Compounds, 2011, 509, 8912-8916.	5.5	11
767	Comparison of hydrogen storage properties of Mg–Ni from different preparation methods. Materials Chemistry and Physics, 2011, 127, 405-408.	4.0	11
768	Binderâ€Free 3D Integrated Ni@Ni 3 Pt Air Electrode for Zn–Air Batteries. Global Challenges, 2019, 3, 1900027.	3.6	11
769	Phosphorusâ€Modulationâ€Triggered Surface Disorder in Titanium Dioxide Nanocrystals Enables Exceptional Sodiumâ€Storage Performance. Angewandte Chemie, 2019, 131, 4062-4066.	2.0	11
770	Electrocatalytic-driven compensation for sodium ion pouch cell with high energy density and long lifespan. Energy Storage Materials, 2021, 39, 54-59.	18.0	11
771	Effect of silver addition on superconductivity in the Bi1.6Pb0.4Sr1.6Ca2Cu3O10?y system. Journal of Materials Science: Materials in Electronics, 1990, 1, 30-33.	2.2	10
772	Effects of substitution for Cu in CuO2planes with dopants of different electron configuration in YBa2Cu3O7. Journal of Physics Condensed Matter, 1993, 5, 3623-3634.	1.8	10
773	Silver-doping effects on the multiple-transition of the complex susceptibility and superconducting properties of melt-textured YBa2Cu3Oymaterials. Superconductor Science and Technology, 1993, 6, 315-321.	3.5	10
774	Mechanism of deformation and "sandwich―rolling process in Ag-clad Bi-based composite tapes. Applied Superconductivity, 1995, 3, 599-605.	0.5	10

#	Article	IF	CITATIONS
775	Electrode properties of Mg2Ni alloy ball-milled with cobalt powder. Electrochimica Acta, 1998, 44, 353-355.	5.2	10
776	Mg2Ni alloy for metal hydride electrodes. Journal of Materials Science, 1998, 33, 4671-4675.	3.7	10
777	The Electrode Properties of Mg[sub 1.9]Al[sub 0.1]Ni[sub 0.8]Co[sub 0.1]Mn[sub 0.1] Alloy by Mechanical Grinding with Ni Powders. Electrochemical and Solid-State Letters, 1999, 2, 164.	2.2	10
778	Stoichiometry-controlled high-performance LiCoO2 electrode materials prepared by a spray solution technique. Journal of Power Sources, 2003, 119-121, 195-200.	7.8	10
779	Enhanced performance of VRLA batteries with a novel spirally-wound electrode design. Journal of Power Sources, 2003, 113, 241-244.	7.8	10
780	Microstructures and Enhancement of Critical Current Density in <tex>\$rm YBa_2rm Cu_3rm O_7\$</tex> Thin Films Grown by Pulsed Laser Deposition on Various Single Crystal Substrates Modified by Ag Nano-Dots. IEEE Transactions on Applied Superconductivity, 2005, 15, 3046-3049.	1.7	10
781	Self-Oriented Ca[sub 3]Co[sub 4]O[sub 9] Thin Film as an Anode Material for Enhanced Cycling Stability of Lithium-Ion Batteries. Electrochemical and Solid-State Letters, 2009, 12, A176.	2.2	10
782	Cocore–Ptshell nanoparticles as cathode catalyst for PEM fuel cells. Journal of Solid State Electrochemistry, 2012, 16, 1105-1110.	2.5	10
783	Lithium rich and deficient effects in LixCoPO4 (x=0.90, 0.95, 1, 1.05) as cathode material for lithium-ion batteries. Electrochimica Acta, 2013, 88, 865-870.	5.2	10
784	Ultrathin Porous NiO Nanoflake Arrays on Nickel Foam as Binder-free Electrodes for Supercapacitors. Electrochemistry, 2016, 84, 219-223.	1.4	10
785	Improved cycling stability of lithium–sulphur batteries by enhancing the retention of active material with a sandwiched hydrothermally treated graphite film. RSC Advances, 2016, 6, 34131-34136.	3.6	10
786	Electrochemical Deposition of Porous VO _x and MnO ₂ Nanowires on Stainless Steel Mesh for Flexible Supercapacitors. Advanced Science Letters, 2010, 3, 295-298.	0.2	10
787	Effect of Annealing on Electrochemical Performance of Anodized TiO ₂ Nanotubes for Lithium Ion Batteries. Advanced Science Letters, 2011, 4, 469-473.	0.2	10
788	The typical structural evolution of silicon anode. Cell Reports Physical Science, 2022, 3, 100811.	5.6	10
789	Flux pinning in Ag-clad (Bi,Pb)2Sr2Ca2Cu3O10+y tape. Solid State Communications, 1994, 92, 735-739.	1.9	9
790	Development of Bi(Pb)-2223/Ag pancake-shaped and solenoidal coils. IEEE Transactions on Applied Superconductivity, 1996, 6, 102-105.	1.7	9
791	Flux pinning in high-Jc tape. Solid State Communications, 1996, 97, 339-343.	1.9	9
792	Properties of Zr0.5Ti0.5(V0.25Mn0.15Ni0.6)2 alloy ball-milled with nickel powder. Journal of Alloys and Compounds, 1997, 248, 146-150.	5.5	9

#	Article	IF	CITATIONS
793	Long lengths of silver-clad Bi2223 superconducting tapes with high current-carrying capacity. Applied Superconductivity, 1997, 5, 163-170.	0.5	9
794	Spiral growth of Bi 2 Sr 2 CaCu 2 O y single crystals using KCl flux technique. Journal of Crystal Growth, 1997, 173, 380-385.	1.5	9
795	Recrystallization effects and grain size in Bi-2223 tapes. Superconductor Science and Technology, 1998, 11, 1082-1086.	3.5	9
796	Effect of various mechanical deformation processes on critical current density and microstructure in MgB2tapes and wires. Superconductor Science and Technology, 2002, 15, 1490-1493.	3.5	9
797	Potential Application of Solid Electrolyte P11 OH in Ni/MH Batteries. Synthetic Metals, 2005, 152, 57-60.	3.9	9
798	In-situ fabrication and characterisation of nanostructured Mn3O4 powders for electronic and electrochemical applications. Materials Letters, 2007, 61, 3189-3192.	2.6	9
799	Preparation of Low Loading Pt/C Catalyst by Carbon Xerogel Method for Ethanol Electrooxidation. Catalysis Letters, 2008, 122, 111-114.	2.6	9
800	Synthesis and characterization of SrBi4Ti4O15ferroelectric filler based composite polymer electrolytes for lithium ion batteries. Polymer Bulletin, 2008, 60, 351-361.	3.3	9
801	Magnetic properties and magnetocaloric effect of (Mn1-xNix)3Sn2(x=0–0.5) compounds. Journal of Applied Physics, 2009, 105, .	2.5	9
802	Enhanced capacity and cycle life of nitrogen-doped activated charcoal anode for the lithium ion battery: a solvent-free approach. RSC Advances, 2017, 7, 16505-16512.	3.6	9
803	Tubular TiO ₂ Nanostructures: Toward Safer Microsupercapacitors. Advanced Materials Technologies, 2018, 3, 1700194.	5.8	9
804	Nanoarchitectured Nitrogen-Doped Graphene/Carbon Nanotube as High Performance Electrodes for Solid State Supercapacitors, Capacitive Deionization, Li-Ion Battery, and Metal-Free Bifunctional Electrocatalysis. ACS Applied Energy Materials, 0, , .	5.1	9
805	A conductive polymer derived N-doped carbon nanofiber supported Li2S coating layer for Li–S batteries with high mass loading. Journal of Alloys and Compounds, 2020, 828, 154264.	5.5	9
806	Phase changes in Y1Ba2Cu3O7-xinduced by Fe2O3and V2O5dopants. Journal of Physics C: Solid State Physics, 1988, 21, L127-L131.	1.5	8
807	Crystallite alignment of YBa2Cu3O7-xthrough texture growth. Superconductor Science and Technology, 1989, 2, 212-215.	3.5	8
808	Mechanism of the Tc enhancement in Bi2Sr2CaCu2O8+y by sodium doping. Physica C: Superconductivity and Its Applications, 1991, 185-189, 811-812.	1.2	8
809	Characterization of Ag-sheathed (Bi,Pb)2Sr2Ca2Cu3O10-x multifilamentary tapes. Cryogenics, 1992, 32, 1038-1041.	1.7	8
810	Differential resistance and critical current distribution in an Ag-clad (BiPb)2Sr2Ca2Cu3O10+y tape. Solid State Communications, 1993, 88, 241-244.	1.9	8

#	Article	IF	CITATIONS
811	Effect of silver on phase formation and superconducting properties of Bi-2223/Ag tapes. IEEE Transactions on Applied Superconductivity, 1995, 5, 1830-1833.	1.7	8
812	Improved critical current of superconducting Bi2223 - Ag tapes for current lead application by addition of `large' silver particles. Superconductor Science and Technology, 1996, 9, 888-892.	3.5	8
813	(Bi, Pb)2Sr2Ca2Cu3O10+x Ag-clad high-Tc superconducting coil and its magnetic field properties. The Philosophical Magazine: Physics of Condensed Matter B, Statistical Mechanics, Electronic, Optical and Magnetic Properties, 1997, 75, 813-826.	0.6	8
814	The formation mechanism and the development of grain texture in the preparation of Ag-sheathed Bi-2223 superconducting tapes. Superconductor Science and Technology, 1998, 11, 770-776.	3.5	8
815	Cryogenic deformation process of high temperature superconductors. Superconductor Science and Technology, 1998, 11, 781-787.	3.5	8
816	Effect of the phase compositions at the final stage of heat treatment on the critical current density in Bi:2223/Ag tapes. Superconductor Science and Technology, 1998, 11, 1057-1060.	3.5	8
817	Visualization of magnetic flux distribution in Bi(Pb)-2223/Ag multifilamentary tapes. Superconductor Science and Technology, 1998, 11, 1017-1023.	3.5	8
818	Enhancement of vortex pinning by Josephson coupling of two-dimensional pancake vortices in heavy lead-doped Bi2-xPbxSr2CaCu2Oy. Superconductor Science and Technology, 2001, 14, 479-485.	3.5	8
819	Comparative studies on "sandwich" rolling and flat rolling in processing Ag/Bi-2223 tapes. IEEE Transactions on Applied Superconductivity, 2001, 11, 3752-3755.	1.7	8
820	AC susceptibility of type-II superconductor strips with geometric barrier. Physica C: Superconductivity and Its Applications, 2002, 377, 416-420.	1.2	8
821	Characterization of Nanoparticles of LiMn ₂ O ₄ Synthesized by a One-Step Intermediate-Temperature Solid-State Reaction. Journal of Nanoscience and Nanotechnology, 2004, 4, 162-166.	0.9	8
822	The morphology, periodical modulation structure and effects of heat treatment on the superconductivity of (Tl, Pb)(Sr, Ba)-1223 single crystals. Superconductor Science and Technology, 2004, 17, 696-700.	3.5	8
823	Improvement of critical current density and thermally assisted individual vortex depinning in pulsed-laser-deposited YBa2Cu3O7â°îſ thin films on SrTiO3 (100) substrate with surface modification by Ag nanodots. Journal of Applied Physics, 2005, 97, 10B107.	2.5	8
824	Hydrothermal synthesis of nanostructured MnO2 under magnetic field for rechargeable lithium batteries. Journal of Solid State Electrochemistry, 2010, 14, 1743-1747.	2.5	8
825	Enhanced Electrochemical Performance of MoS ₂ for Lithium Ion Batteries by Simple Chemical Lithiation. Journal of the Chinese Chemical Society, 2012, 59, 1196-1200.	1.4	8
826	High performance pure sulfur honeycomb-like architectures synthesized by a cooperative self-assembly strategy for lithium–sulfur batteries. RSC Advances, 2014, 4, 36513-36516.	3.6	8
827	Hydrogels: Edgeâ€Hydroxylated Boron Nitride Nanosheets as an Effective Additive to Improve the Thermal Response of Hydrogels (Adv. Mater. 44/2015). Advanced Materials, 2015, 27, 7247-7247.	21.0	8
828	Effect of Sn substitution for Co on microstructure and electrochemical performance of AB5 type La0.7Mg0.3Al0.3Mn0.4Co0.5–xSnxNi3.8 (x=0–0.5) alloys. Transactions of Nonferrous Metals Society of China, 2015, 25, 520-526.	4.2	8

#	Article	IF	CITATIONS
829	Mass Production and Pore Size Control of Holey Carbon Microcages. Angewandte Chemie, 2017, 129, 13978-13982.	2.0	8
830	Rapid hydrothermal synthesis of Li3VO4 with different favored facets. Journal of Solid State Electrochemistry, 2017, 21, 2547-2553.	2.5	8
831	Dependence of the Superconducting Transition Temperature on Radii of Alkali and Alkaline Earth Dopants in Y ₁ Ba ₂ Cu ₃ O _{7â^x} . Physica Status Solidi (B): Basic Research, 1988, 147, K153.	1.5	7
832	Enhanced flux pinning through a phase formation-decomposition-recovery process in Ag-sheathed Bi(Pb)SrCaCuO wires. IEEE Transactions on Applied Superconductivity, 1993, 3, 1135-1138.	1.7	7
833	Vortex state and flux pinning in Bi2223/Ag tape. Solid State Communications, 1995, 95, 515-518.	1.9	7
834	Scaling of Jc-B curves in BSCCO/Ag tapes. Solid State Communications, 1996, 100, 187-190.	1.9	7
835	On the discharging process of titanium-based hydrogen storage alloy electrode via a.c. impedance analysis. Journal of Power Sources, 1996, 62, 75-79.	7.8	7
836	High temperature superconducting magnetic levitation train. Applied Superconductivity, 1997, 5, 201-204.	0.5	7
837	Morphologies of square shape spirals and (110) twins in spiral-grown Bi2Sr2CaCu2Oy crystals. Physica C: Superconductivity and Its Applications, 1997, 273, 349-353.	1.2	7
838	Magnetic separation techniques and HTS magnets. Superconductor Science and Technology, 1998, 11, 1071-1074.	3.5	7
839	Fabrication and properties of some Ag-alloy sheathed Bi-2223 tapes. IEEE Transactions on Applied Superconductivity, 1999, 9, 2710-2713.	1.7	7
840	Transmission electron microscopy evidence for phase transformation from Bi2Sr2CuO6 to Bi2Sr2Ca2Cu3O10. Applied Physics Letters, 2002, 81, 688-690.	3.3	7
841	Characterization of thermal conductivity and mechanical properties of Ag-alloy sheathed Bi(Pb)-Sr-Ca-Cu-O superconductor tape. IEEE Transactions on Applied Superconductivity, 2003, 13, 2956-2959.	1.7	7
842	Influence of Ca ₂ PbO ₄ on Phase Formation and Electrical Properties of (Bi,Pb) ₂ Sr ₂ Ca ₂ Cu ₃ O ₁₀ /Ag Superconducting Composites. Journal of the American Ceramic Society, 2000, 83, 1675-1680.	3.8	7
843	Electron Transfer Behavior of Monolayer Protected Nanoclusters and Nanowires of Silver and Gold. Journal of Nanoscience and Nanotechnology, 2006, 6, 3464-3469.	0.9	7
844	Effects of milling conditions on hydrogen storage properties of graphite. Journal of Materials Science, 2007, 42, 5437-5441.	3.7	7
845	Hydrogen Storage Properties of Mg-BCC Composite. International Journal of Green Energy, 2009, 6, 607-615.	3.8	7
846	Nanostructured Metal Oxides as Electrode Materials for Electrochemical Capacitors. Journal of Nanoscience and Nanotechnology, 2009, 9, 1263-1267.	0.9	7

#	Article	IF	CITATIONS
847	Tin Oxide Thin Film with Threeâ€Dimensional Ordered Reticular Morphology as a Lithium Ion Battery Anode. ChemPhysChem, 2009, 10, 3101-3104.	2.1	7
848	Electrochemical properties of Fe ₂ O ₃ thin film fabricated by electrostatic spray deposition for lithium-ion batteries. Physica Scripta, 2010, T139, 014066.	2.5	7
849	Synthesis and modification of non-stoichiometric spinel (Li1.02Mn1.90Y0.02O4â^'yF0.08) for lithium-ion batteries. Materials Chemistry and Physics, 2010, 119, 82-85.	4.0	7
850	Self-monitoring and self-correcting polymer fibers coated with carbon nanotubes. Carbon, 2016, 109, 428-434.	10.3	7
851	Hybrids of Fe3O4/CoSe2 as efficient electrocatalysts for oxygen reduction reaction. Journal of Materials Science, 2018, 53, 1123-1134.	3.7	7
852	An in-situ generated Bi-based sodiophilic substrate with high structural stability for high-performance sodium metal batteries. Journal of Energy Chemistry, 2022, 71, 595-603.	12.9	7
853	Twins, kinks and cracks in dense superconducting YBa2Cu3O7â^'x. Journal of Materials Science Letters, 1989, 8, 1147-1150.	0.5	6
854	Long multifilament Bi-2223 Ag-sheathed superconducting tapes and solenoids. Journal of Superconductivity and Novel Magnetism, 1994, 7, 829-833.	0.5	6
855	Mössbauer study of a novel series of ternary rare-earth iron-rich intermetallics: ND(Fe1-xTi x)6+y(x â^¼) Tj ET	Qq110.78	4314 rgBT /
856	Equilibrium phase diagrams in the system CuO–PbO–Ag. Journal of Materials Research, 1995, 10, 2933-2937.	2.6	6
857	Effect of rolling reduction on the transport property, microstructure, phase formation and fill factor of high-Tc superconducting Bi-(Pb)-Sr-Ca-Cu-O tapes. Cryogenics, 1996, 36, 903-913.	1.7	6
858	-B-Tsurface of high- tape. Superconductor Science and Technology, 1996, 9, 1060-1065.	3.5	6
859	Effect of final annealing temperature on critical current density of Ag/Bi-(Pb)-Sr-Ca-Cu-O tapes. Applied Superconductivity, 1997, 5, 171-177.	0.5	6
860	Influence of bismuth on hydrogen and oxygen evolution on lead-calcium-tin-aluminium grid alloys. Journal of Power Sources, 1997, 66, 159-164.	7.8	6
861	Design, fabrication and properties of 1 T (4.2 K) Bi-2223 high- superconducting prototype magnet. Superconductor Science and Technology, 1998, 11, 535-539.	3.5	6
862	Vapour cooled high current leads utilizing Bi-2223/Ag tapes. Superconductor Science and Technology, 1998, 11, 1091-1094.	3.5	6
863	A high gradient magnetic separator fabricated using Bi-2223/Ag HTS tapes. IEEE Transactions on Applied Superconductivity, 1999, 9, 394-397.	1.7	6
864	Orientation Distribution of Grain Planes in Polycrystal Ag/Bi-2223 Tape. Journal of Superconductivity and Novel Magnetism, 2000, 13, 441-446.	0.5	6

#	Article	IF	CITATIONS
865	Optimized NdBa2Cu3Oy thin films deposited by eclipsed pulsed laser ablation. Physica C: Superconductivity and Its Applications, 2001, 356, 205-211.	1.2	6
866	A new process for fabrication of metal-hydride electrodes for nickel–metal hydride batteries. Journal of Alloys and Compounds, 2002, 330-332, 760-765.	5.5	6
867	Lead-coated glass fibre mesh grids for lead–acid batteries. Journal of Applied Electrochemistry, 2003, 33, 1057-1061.	2.9	6
868	Electrochemical and in situ synchrotron X-ray diffraction studies of Li[Li0.3Cr0.1Mn0.6]O2 cathode materials. Solid State Ionics, 2004, 167, 183-189.	2.7	6
869	Fluorine: Edge-Fluorinated Graphene Nanoplatelets as High Performance Electrodes for Dye-Sensitized Solar Cells and Lithium Ion Batteries (Adv. Funct. Mater. 8/2015). Advanced Functional Materials, 2015, 25, 1328-1328.	14.9	6
870	Synthesis and electrochemical properties of NH 4 FePO 4 ·H 2 O as a novel anode material. Materials Letters, 2018, 225, 69-72.	2.6	6
871	Pt/C Catalysts Using Different Carbon Supports for the Cathode of PEM Fuel Cells. Advanced Science Letters, 2011, 4, 115-120.	0.2	6
872	Nanosize SnO2 for Highly Responsive Gas Sensor Application. Sensor Letters, 2010, 8, 243-246.	0.4	6
873	Conductor design with high-Tc superconducting Bi(Pb)—2223/Ag multifilamentary tapes. Materials Science and Engineering B: Solid-State Materials for Advanced Technology, 1996, 40, 217-223.	3.5	5
874	Effect of sintering temperature on phase composition and J/sub c/ of Ag-sheathed Bi-2223 single and multifilamentary tapes. IEEE Transactions on Applied Superconductivity, 1997, 7, 1845-1848.	1.7	5
875	Comparative study of electrochemical behaviour of single-crystalline and polycrystalline LaNi5 alloy electrodes. Journal of Alloys and Compounds, 1997, 248, 159-163.	5.5	5
876	The oxygenation processes of YBa2Cu3O6+ with silver additions. Physica C: Superconductivity and Its Applications, 1998, 303, 202-208.	1.2	5
877	Colossal and constant magnetoresistance over a large temperature range between 230 and 4.2 K in La0.8Li0.2MnO3 prepared by a partial melting technique. Journal of Alloys and Compounds, 1998, 270, L10-L12.	5.5	5
878	An electrometric method for evaluation of the corrosion of lead alloys. Journal of Power Sources, 1999, 77, 56-63.	7.8	5
879	Effect of the sinter-forging deformation rate on properties of Bi-2223 current leads. IEEE Transactions on Applied Superconductivity, 2001, 11, 2551-2554.	1.7	5
880	Nanocrystalline <i>α</i> -Ni(OH) ₂ Prepared by Ultrasonic Precipitation. Journal of Nanoscience and Nanotechnology, 2002, 2, 45-46.	0.9	5
881	Third harmonics due to surface barrier in high-temperature superconductor. Journal of Applied Physics, 2005, 97, 10B105.	2.5	5
882	In situ high temperature optical microscopy study of phase evolution in YBa2Cu3O7â^'î´ films prepared by a fluorine-free sol–gel route. Physica C: Superconductivity and Its Applications, 2006, 436, 62-67.	1.2	5

#	Article	IF	CITATIONS
883	Highly oriented LiFePO4 thin film electrodes via chemical solution deposition. Solid State Ionics, 2014, 268, 117-124.	2.7	5
884	Effects of Reducing Temperatures on the Hydrogen Storage Capacity of Double-Walled Carbon Nanotubes with Pd Loading. Journal of Nanoscience and Nanotechnology, 2014, 14, 4706-4709.	0.9	5
885	Self-assembling RuO ₂ nanogranulates with few carbon layers as an interconnected nanoporous structure for lithium–oxygen batteries. Chemical Communications, 2020, 56, 7253-7256.	4.1	5
886	Stable sodium metal anodes enabled by an in-situ generated mixed-ion/electron-conducting interface. Chemical Engineering Journal, 2022, 446, 136917.	12.7	5
887	Processing, characterisation and properties of the superconducting Tl-Ba-Ca-Cu-O system. Superconductor Science and Technology, 1988, 1, 83-87.	3.5	4
888	Superlattices and stacking faults in Bi ₂ (Sr,) Tj ETQq0 0 0 rgBT /Overlock 10 Tf 50 542 Td (Ca)	3C	u ₂
889	T(I)-O-T(II) structural transition and superconductivity in the Sr-based 123 compounds YSr2Cu2.8Mo0.1W0.1Oy. Solid State Communications, 1993, 88, 813-819.	1.9	4
890	Intrinsic critical current of Ag-clad (Bi,Pb)2Sr2Ca2Cu3O z tapes. Journal of Superconductivity and Novel Magnetism, 1994, 7, 809-812.	0.5	4
891	Compensation effect, impurity scattering and superconductivity in 123 compounds. Physica B: Condensed Matter, 1994, 194-196, 1957-1958.	2.7	4
892	Field, temperature, and angle dependence of the critical current density in Bi2Sr2CaCu2O10/Ag ribbons. Journal of Superconductivity and Novel Magnetism, 1995, 8, 37-42.	0.5	4
893	Structure and magnetic properties of the ternary compound. Journal of Physics Condensed Matter, 1996, 8, 2881-2886.	1.8	4
894	Effect on critical current density and irreversibility behaviour of mechanical deformation of Bi-(Pb)-Sr-Ca-Cu-O superconducting tapes. IEEE Transactions on Applied Superconductivity, 1997, 7, 1841-1844.	1.7	4
895	The effect of ball milling and rapid quenching on the catalytic activity of the Cu30Al70 alloy. Materials Letters, 1997, 33, 79-83.	2.6	4
896	Effect of Cu-site Co, Ni and Ga substitution on the superconductivity of tetragonal LaBaCaCu3O7 system. Physica C: Superconductivity and Its Applications, 1998, 301, 205-214.	1.2	4
897	The effect of Zn(OH)2 addition on the electrode properties of nickel hydroxide electrodes. Journal of Materials Research, 1999, 14, 1916-1921.	2.6	4
898	Significantly enhanced critical current density in Bi-2223/Ag multifilamentary tapes by hot pressing. IEEE Transactions on Applied Superconductivity, 1999, 9, 2742-2745.	1.7	4
899	Magneto-optical images of Ag/Bi-2223 tapes processed by flat rolling, "sandwich" rolling and pressing. IEEE Transactions on Applied Superconductivity, 2001, 11, 3764-3767.	1.7	4
900	Effect of Ti Doping on the Superconductivities of MgB2/Fe Wires. Journal of Low Temperature Physics, 2003, 131, 687-692.	1.4	4

#	Article	IF	CITATIONS
901	Magnetic flux distribution in a superconducting core of Bi-2223 tape. Physica C: Superconductivity and Its Applications, 2003, 388-389, 405-406.	1.2	4
902	A novel cureless paste for positive plates in valve-regulated batteries. Journal of Power Sources, 2003, 122, 195-200.	7.8	4
903	Effects of the field dependent J/sub c/ on the vertical levitation force between a superconductor and a magnet. IEEE Transactions on Applied Superconductivity, 2003, 13, 2142-2145.	1.7	4
904	Calculation of the temperature dependent AC susceptibility of superconducting disks. IEEE Transactions on Applied Superconductivity, 2003, 13, 3742-3745.	1.7	4
905	Thermal stability and hydrogen storage property of Mg1.9Cu0.1Nix (x=1.8, 1.9, 2.0 and 2.1) alloys. Journal of Alloys and Compounds, 2006, 426, 335-340.	5.5	4
906	SYNTHESIS OF NANO-CRYSTALLINE CO3O4 PARTICLES BY HYDROTHERMAL METHOD UNDER PULSED MAGNETIC FIELD. International Journal of Modern Physics B, 2009, 23, 3602-3607.	2.0	4
907	Preparation of tin nanocomposite as anode material by molten salts method and its application in lithium ion batteries. Physica Status Solidi (A) Applications and Materials Science, 2009, 206, 2546-2550.	1.8	4
908	Electrochemical Performance of Nanocrystalline SnO ₂ -Carbon Nanotube Composites as Anode in Lithium-Ion Cells. Journal of Nanoscience and Nanotechnology, 2009, 9, 1474-1478.	0.9	4
909	Rietveld Analysis of the Effect of Annealing Atmosphere on Phase Evolution of Nanocrystalline TiO ₂ Powders. Journal of Nanoscience and Nanotechnology, 2012, 12, 4724-4728.	0.9	4
910	One-Step Spray Pyrolysis Synthesized CuO-Carbon Composite Combined with Carboxymethyl Cellulose Binder as Anode for Lithium-Ion Batteries. Journal of Nanoscience and Nanotechnology, 2012, 12, 1314-1317.	0.9	4
911	Design of selfâ€assembled TiO ₂ architectures: Towards hybrid nanotubular interfaces. Physica Status Solidi (A) Applications and Materials Science, 2014, 211, 938-945.	1.8	4
912	A triblock-copolymer-templating route to carbon spheres@SBA-15 large mesopore core–shell and hollow structures. RSC Advances, 2014, 4, 48676-48681.	3.6	4
913	Effects of Cu Substitution for Sn on the Electrochemical Performance of La0.7Mg0.3Al0.3Mn0.4Sn0.5â^'xCuxNi3.8 (x = 0–0.5) Alloys for Ni-MH Batteries. Batteries, 2015, 1, 3-10.	4.5	4
914	Effective enhancement of the electrochemical performance of layered cathode Li _{1.5} Mn _{0.75} Ni _{0.25} O _{2.5} via a novel facile molten salt method. RSC Advances, 2015, 5, 58528-58535.	3.6	4
915	Influence of nonlinear charge transfer on the behaviour of the mobile hole concentration and Tcin the YBa2Cu3O7-ysystem. Superconductor Science and Technology, 1992, 5, 295-298.	3.5	3
916	On the superconductivity suppression in the oxide systems Y1â^'x Pr x Ba2Cu3â^'y MyOz (M = Zn and Al). Physics Letters, Section A: General, Atomic and Solid State Physics, 1993, 177, 437-440.	2.1	3
917	Microstructures of high-J c melt-textured YBa2Cu3O7?x /Ag superconductors. Journal of Superconductivity and Novel Magnetism, 1994, 7, 947-950.	O.5	3
918	Construction and normal zone propagation analysis of high-T/sub c/ superconducting Bi(Pb)-2223/Ag class II coils and magnets. IEEE Transactions on Applied Superconductivity, 1997, 7, 893-895.	1.7	3

#	Article	IF	CITATIONS
919	Surface-modified Mg/sub 2/Ni-type negative electrode materials for Ni-MH battery. , 0, , .		3
920	The oxygenation kinetics of -(0-30%)Ag superconductors. Superconductor Science and Technology, 1998, 11, 1193-1199.	3.5	3
921	Softening of Bi2212 crystals and growth mechanism of Bi2212 and Bi2201 grown at the KCl flux surface. Superconductor Science and Technology, 1999, 12, 77-80.	3.5	3
922	General design formula for tapered, conduction-cooled current lead utilizing high temperature superconducting tapes. Superconductor Science and Technology, 1999, 12, 181-183.	3.5	3
923	Title is missing!. Journal of Applied Electrochemistry, 1999, 29, 177-183.	2.9	3
924	A Modal of Twin Domains in YBa2(Cu1â^'xCox)3Oy. Journal of Superconductivity and Novel Magnetism, 2000, 13, 129-136.	0.5	3
925	Fabrication and Properties of Spray-Dried Nanofeatured Spherical Ni(OH) ₂ Materials. Journal of Nanoscience and Nanotechnology, 2002, 2, 675-678.	0.9	3
926	The peak effect in Fe-doped Bi-2212 single crystals. Superconductor Science and Technology, 2002, 15, 356-360.	3.5	3
927	AC response studying on MgB2 superconductor by Maley's method. Physica C: Superconductivity and Its Applications, 2003, 386, 631-637.	1.2	3
928	A comparison of ag and Ag-alloy sheathed Bi-2223 tapes. IEEE Transactions on Applied Superconductivity, 2003, 13, 3004-3007.	1.7	3
929	Study of Oxygen Incorporation in PLD \${m MgB}_{2}\$ Films by Rutherford Backscattering Spectroscopy. IEEE Transactions on Applied Superconductivity, 2007, 17, 2875-2878.	1.7	3
930	DSC study of the effect of milling conditions on the hydrogen storage properties of boron. Journal of Materials Science, 2007, 42, 3985-3989.	3.7	3
931	Synthesis and Electrochemical Studies on Li2CuSnO4 and Li2CuSnSiO6 as Negative Electrode in the Lithium Batteries. ECS Transactions, 2009, 25, 75-89.	0.5	3
932	Enhanced Cycling Performance of Nanocrystalline Fe ₃ O ₄ /C as Anode Material for Lithium-Ion Batteries. Journal of Nanoscience and Nanotechnology, 2012, 12, 1246-1250.	0.9	3
933	Streamline Sulfur Redox Reactions to Achieve Efficient Roomâ€Temperature Sodium–Sulfur Batteries. Angewandte Chemie, 2022, 134, .	2.0	3
934	Superlattices in Pb-doped Bi-Sr-Ca-Cu-O and in a non-superconducting Sr-Ca-Cu-O precursor. Philosophical Magazine Letters, 1989, 59, 213-217.	1.2	2
935	Phase diagram and microstructure in the system CuO-PbO-Ag. Journal of Superconductivity and Novel Magnetism, 1994, 7, 69-71.	0.5	2
936	Sandwich Roiling, Jc, and pinning energy in Ag-sheathed BPSCCO superconducting tapes. Journal of Electronic Materials, 1995, 24, 1801-1804.	2.2	2

#	Article	IF	CITATIONS
937	Finite voltages along the c-direction of Bi-2223/Ag multifilament tape. Superconductor Science and Technology, 1997, 10, 342-346.	3.5	2
938	Charging efficiency of metal-hydride electrodes. Journal of Power Sources, 1998, 70, 110-113.	7.8	2
939	High electrical performance Ag-sheathed Bi-2223 multifilamentary tapes prepared by an optimised PIT processing route. IEEE Transactions on Applied Superconductivity, 1999, 9, 2730-2733.	1.7	2
940	Effect of cryogenic deformation on microstructure and critical current density in Ag/Bi-2223 tapes. IEEE Transactions on Applied Superconductivity, 1999, 9, 2726-2729.	1.7	2
941	Development of long length Bi-based/Ag tapes and experimental magnets. IEEE Transactions on Applied Superconductivity, 1999, 9, 2605-2608.	1.7	2
942	The flux pinning potential of Ag/Bi-2223 tapes for H//c-axis. Physica C: Superconductivity and Its Applications, 2000, 341-348, 1353-1354.	1.2	2
943	Upper Critical Field Hc2 on c Axis of Ag/Bi-2223 Polycrystal Tape. Journal of Superconductivity and Novel Magnetism, 2001, 14, 465-468.	O.5	2
944	Phase transformation characteristics of BSCCO tapes processed via cryogenic and room temperature pressing. Superconductor Science and Technology, 2001, 14, 533-538.	3.5	2
945	Comparison studies of spiral growth mechanism in Bi2Sr2CaCu2Oy and YBa2Cu3Oy high temperature superconducting single crystals. International Journal of Modern Physics B, 2002, 16, 9-18.	2.0	2
946	Effects of grain size and grain boundaries on the transport and magnetic properties of charge-ordered Nd0.5Sr0.5MnO3material. Superconductor Science and Technology, 2002, 15, 423-426.	3.5	2
947	Synthesis of functional oxides by a novel mechanical milling–electric discharge method. Journal of Materials Chemistry, 2006, 16, 4488-4493.	6.7	2
948	Enhanced electrochemical properties of nonstoichiometric amorphous Mg2Ni1.3 electrodes. Journal of Applied Electrochemistry, 2006, 36, 11-16.	2.9	2
949	Real-time measurement of desorption temperature and kinetics of magnesium hydride powder sample based on optical reflection. International Journal of Hydrogen Energy, 2009, 34, 9168-9172.	7.1	2
950	Foam-like, microstructural SnO ₂ –carbon composite thin films synthesized via a polyol-assisted thermal decomposition method. Dalton Transactions, 2009, , 723-729.	3.3	2
951	Lithium–Oxygen Batteries: Porous AgPd–Pd Composite Nanotubes as Highly Efficient Electrocatalysts for Lithium–Oxygen Batteries (Adv. Mater. 43/2015). Advanced Materials, 2015, 27, 7012-7012.	21.0	2
952	Lithiumâ€lon Batteries: A Green and Facile Way to Prepare Granadillaâ€Like Siliconâ€Based Anode Materials for Liâ€lon Batteries (Adv. Funct. Mater. 3/2016). Advanced Functional Materials, 2016, 26, 468-468.	14.9	2
953	Sodium–Sulfur Batteries: Remedies for Polysulfide Dissolution in Roomâ€Temperature Sodium–Sulfur Batteries (Adv. Mater. 18/2020). Advanced Materials, 2020, 32, 2070145.	21.0	2
954	60 K superconductivity in a Y1-xCaxBa2Cu3-xAlxO6.35system-a possible local hole effect. Superconductor Science and Technology, 1992, 5, 569-574.	3.5	1

#	Article	IF	CITATIONS
955	Magnetic field dependence of the critical current density for the bismuth-based bulk high-Tc superconductors. Journal of Materials Science, 1992, 27, 3043-3049.	3.7	1
956	Novel ternary iron-rich, rare-earth iron silicides: R3(Fe1â^'x Si x)22 (x â^¼ 0.16). Hyperfine Interactions, 1994, 94, 1921-1927.	0.5	1
957	Fabrication of Ag-sheathed Bi-superconducting tapes and coils. IEEE Transactions on Applied Superconductivity, 1995, 5, 1267-1270.	1.7	1
958	Critical current densities of high-Tc Bi(Pb)-2223 wire-in-tube, continuous-tube-forming/filling and silver-alloy double-pancake coils at 77 K. Applied Superconductivity, 1996, 4, 343-347.	0.5	1
959	Comparative studies on single crystals and superconducting Bi-(Pb)-Sr-Ca-Cu-O tapes. IEEE Transactions on Applied Superconductivity, 1997, 7, 2219-2222.	1.7	1
960	Studies on the electrochemical impedance spectroscopy of Zr-based Laves phase metal hydride electrodes. , 0, , .		1
961	Multi-spirals in spiral grown Bi2Sr2CaCu2Oy crystals. Journal of Materials Science Letters, 1997, 16, 858-859.	0.5	1
962	Development of high energy nickel-metal hydride cell. , 0, , .		1
963	Silver-clad superconducting tapes fabricated by different mechanical processing. Superconductor Science and Technology, 1998, 11, 1053-1056.	3.5	1
964	Fabrication and Characterization of High-T _c Superconducting Continuous-Tube-Forming/Filling Bi(Pb)-2223/Ag Composites and Coils. Materials and Manufacturing Processes, 1998, 13, 337-357.	4.7	1
965	Structural and electrochemical characteristics of Li/sub 1+x/Mn/sub 2+x/O/sub 4/ and LiMn/sub 2/O/sub 4-Î′/ for secondary lithium batteries. , 0, , .		1
966	The effect of deformation reduction in hot-pressing on critical current density of (Bi,) Tj ETQq0 0 0 rgBT /Overlock 2455-2456.	10 Tf 50 1.2	307 Td (Pb)2 1
967	Pinning characteristics of MgB2near the melting curve. Superconductor Science and Technology, 2002, 15, 619-623.	3.5	1
968	Transverse micro- and mesotexture distribution characteristics on the core surface of (Bi,Pb)2Sr2Ca2Cu3O10/Ag superconductor tape. Superconductor Science and Technology, 2002, 15, 241-246.	3.5	1
969	Effect of substrate surface modification using Ag nano-dots on the improvement of J c and microstructures in YBa2Cu3O7 thin films grown on LaAlO3 (100) by pulsed laser deposition. Journal of Electroceramics, 2006, 16, 605-609.	2.0	1
970	Microstructure Observations of Ag and Ag-Alloy Sheathed Bi2223 Tapes. IEEE Transactions on Applied Superconductivity, 2007, 17, 3095-3098.	1.7	1
971	HYDROTHERMAL SYNTHESIS OF NANOCRYSTAL MNO ₂ UNDER PULSED MAGNETIC FIELD. International Journal of Modern Physics B, 2009, 23, 3608-3612.	2.0	1
972	Preface for "Lithium ion batteries and beyond― APL Materials, 2018, 6, 047401.	5.1	1

#	Article	IF	CITATIONS
973	Lithium Storage: 3D Selenium Sulfide@Carbon Nanotube Array as Long-Life and High-Rate Cathode Material for Lithium Storage (Adv. Funct. Mater. 43/2018). Advanced Functional Materials, 2018, 28, 1870310.	14.9	1
974	Anode Materials: Realizing Reversible Conversionâ€Alloying of Sb(V) in Polyantimonic Acid for Fast and Durable Lithium―and Potassium―on Storage (Adv. Energy Mater. 1/2020). Advanced Energy Materials, 2020, 10, 2070002.	19.5	1
975	Porous quasi-graphitic carbon sheets for unprecedented sodium storage. Inorganic Chemistry Frontiers, 2020, 7, 2443-2450.	6.0	1
976	Coupling effects of thermodynamics in multiple ion co-precipitation for precursors towards a layered oxide cathode. Materials Advances, 2021, 2, 3752-3759.	5.4	1
977	Acid Treatment of Carbon Supports for Proton Exchange Membrane Fuel Cell Electrocatalyst. Advanced Science Letters, 2011, 4, 492-495.	0.2	1
978	Microstructures, Jcand flux pinning in Ag─Clad Bi─Pb─Sr─Ca─Cu─O wires. Phase Transitions, 1993,	41,39-85	. 0
979	Thermal stability in high-T c coil and magnet design by process control of Bi(Pb)-2223/Ag multifilamentary tapes. Journal of Superconductivity and Novel Magnetism, 1996, 9, 605-614.	0.5	0
980	Irreversible magnetization and critical currents in silver-sheathed (Bi, Pb)2Sr2Ca2Cu3O10 + y tape. Physica Status Solidi A, 1996, 157, 427-437.	1.7	0
981	Microstructure and critical current of hot-pressed (Bi,Pb)/sub 2/Sr/sub 2/Ca/sub 2/Cu/sub 3/O/sub 10/ ceramics. IEEE Transactions on Applied Superconductivity, 1997, 7, 1849-1852.	1.7	0
982	The kinetics of PbSO/sub 4//PbO/sub 2/ on Pb-Ca-Sn-Al grid alloys with bismuth additions at different temperature. , 0, , .		0
983	Properties of chemically prepared MmNi4.52Mn0.49 alloy. Journal of Alloys and Compounds, 1997, 260, 260-264.	5.5	0
984	On the role of Bi2Sr2Ca1Cu2O8 and Bi2Sr2Cu1O6 on the weak links and critical currents in (Bi,Pb)2Sr2Ca2Cu2O10/Ag superconducting tapes. Applied Superconductivity, 1997, 5, 179-185.	0.5	0
985	Magnetization studies and irreversibility behavior of high-Tc superconducting Bi(Pb)-2223 multifilamentary Ag-sheathed PIT tapes prepared from differently synthesized precursor powders. Solid State Communications, 1998, 108, 319-324.	1.9	0
986	Study of microstructures of Ag-sheathed (BiPbSrCaCuO) multifilamentary tapes in various stages of processing. Journal of Materials Research, 1998, 13, 279-283.	2.6	0
987	Comparative studies of the fishtail effect associated with surface pinning and oxygen vacancy network in spiral and layer-by-layer grown single crystals. Superconductor Science and Technology, 1998, 11, 1041-1044.	3.5	0
988	Effect of short processing time on Bi-2223 phase formation kinetics and critical current in Bi-2223/Ag tapes. IEEE Transactions on Applied Superconductivity, 1999, 9, 2734-2737.	1.7	0
989	SMALL ANGLE GRAIN BOUNDARY IN YBa2Cu3Oy SUPERCONDUCTOR. International Journal of Modern Physics B, 1999, 13, 2285-2290.	2.0	0
990	Increase in Tc of YBa2Cu3Oy by oxygen plasma treatment. Physica C: Superconductivity and Its Applications, 2000, 341-348, 2451-2452.	1.2	0

#	Article	IF	CITATIONS
991	Improvement in critical current density of Agî—,Mg alloy sheathed Bi-2223 tapes by cryogenic pressing. Physica C: Superconductivity and Its Applications, 2000, 341-348, 2581-2582.	1.2	0
992	Title is missing!. Journal of Superconductivity and Novel Magnetism, 2000, 13, 633-638.	0.5	0
993	Segregation growth of Bi2(Sr,Ca)2CuOy single crystals by using self-fluxes. Journal of Materials Science Letters, 2001, 20, 1455-1457.	0.5	0
994	Effect of Various Intermediate Deformation Techniques on Jc and Grain Texture for Ag/Bi-2223 Tapes. Journal of Superconductivity and Novel Magnetism, 2001, 14, 539-543.	0.5	0
995	Intrinsic deformation behaviour in pressed Bi-Sr-Ca-Cu-O tapes. Superconductor Science and Technology, 2001, 14, 862-869.	3.5	0
996	Effects of magnetic field on vortex dynamics in (Tl,Pb)(Sr,Ba)2Ca2Cu3Oy single crystal. Physica C: Superconductivity and Its Applications, 2003, 399, 15-21.	1.2	0
997	Magnetic hysteresis and relaxation in Bi2212 single crystals doped with Fe and Pb. IEEE Transactions on Applied Superconductivity, 2003, 13, 3770-3773.	1.7	0
998	The effect of pre-sintering and deformation rate on critical current density behaviour of Bi-2223 bulk samples made by sinter forging. Superconductor Science and Technology, 2003, 16, 804-808.	3.5	0
999	A novel cureless pure lead oxide plate for valve-regulated lead-acid batteries. Journal of Applied Electrochemistry, 2004, 34, 1127-1133.	2.9	0
1000	Various Carbon Metal Nanocomposites for Lithium Ion Batteries and Direct Methanol Fuel Cells. ECS Transactions, 2008, 6, 205-213.	0.5	0
1001	Phase transformation in Bi-2223/AgMg alloyed PIT tapes during different sintering processing and its influence on critical current density. Physica C: Superconductivity and Its Applications, 2008, 468, 2305-2312.	1.2	0
1002	V2O5 Nanorods with Improved Cycling Stability for Li Intercalation. Materials Research Society Symposia Proceedings, 2009, 1170, 76.	0.1	0
1003	Hydrogen Storage Properties of Mg-Ni Alloy Catalysed by Multi-Walled Carbon Nanotubes. Materials Science Forum, 2010, 654-656, 2843-2846.	0.3	0
1004	Characterization of Pd Nano-Thin Films for High-Speed Switchable Mirrors. Materials Science Forum, 0, 700, 166-169.	0.3	0
1005	Corrigendum to "Rapid synthesis of Li4Ti5O12/grapheme composite with superior rate capability by a microwave-assisted hydrothermal method" [Nano Energy (2014) 8, 297–304]. Nano Energy, 2016, 30, 910.	16.0	0
1006	Nanoparticles: Germanium Nanograin Decoration on Carbon Shell: Boosting Lithium-Storage Properties of Silicon Nanoparticles (Adv. Funct. Mater. 43/2016). Advanced Functional Materials, 2016, 26, 7799-7799.	14.9	0
1007	Irradiation Si on Carbon Nanotube Paper as a Flexible Anode Material for Lithium-Ion Batteries. Nanoscience and Nanotechnology Letters, 2012, 4, 169-172.	0.4	0
1008	Building Better Potassium Ion Batteries with Symmetric Electrodes. SSRN Electronic Journal, 0, , .	0.4	0